Toward establishing an abundant B and B_s spectrum up to the second orbital excitations

Qi Li, Ru-Hui Ni, and Xian-Hui Zhong*

Department of Physics, Hunan Normal University, Changsha 410081, China;
Synergetic Innovation Center for Quantum Effects and Applications (SICQEA), Changsha 410081, China,
and Key Laboratory of Low-Dimensional Quantum Structures
and Quantum Control of Ministry of Education, Changsha 410081, China

(Received 23 February 2021; accepted 10 May 2021; published 8 June 2021)

Stimulated by the exciting progress in experiments, we carry out a combined analysis of the masses, and strong and radiative decay properties of the B and B_s-meson states up to the second orbital excitations. Based on our good descriptions of the mass and decay properties for the low-lying well-established states $B_1(5721)$, $B_2^*(5747)$, $B_{s1}(5830)$ and $B_{s2}^*(5840)$, we give a quark model classification for the high mass resonances observed in recent years. It is found that (i) the $B_J(5840)$ resonance may be explained as the low mass mixed state $B(|SD\rangle_L)$ via $2^3S_1 - 1^3D_1$ mixing, or the pure $B(2^3S_1)$ state, or $B(2^1S_0)$. (ii) The $B_J(5970)$ resonance may be assigned as the 1^3D_3 state in the B meson family, although it as a pure 2^3S_1 state cannot be excluded. (iii) The narrow structure around 6064 MeV observed in the B^+K^- mass spectrum at LHCb may be mainly caused by the $B_{sJ}(6109)$ resonance decaying into $B^{*+}K^-$, and favors the assignment of the high mass $1D$-wave mixed state $B_s(1D_2')$ with $J^P = 2^-$, although it as the 1^3D_3 state cannot be excluded. (iv) The relatively broader $B_{sJ}(6114)$ structure observed at LHCb may be explained with the mixed state $B_s(|SD\rangle_H)$ via $2^3S_1 - 1^3D_1$ mixing, or a pure 1^3D_1 state. Most of the missing $1P$-, $1D$-, and $2S$-wave B- and B_s-meson states have a relatively narrow width, they are most likely to be observed in their dominant decay channels with a larger data sample at LHCb.

DOI: 10.1103/PhysRevD.103.116010

I. INTRODUCTION

Since 2007, significant progress has been made in the observations of the bottom and bottom-strange mesons [1]. In 2007, two low-lying orbitally excited narrow B mesons $B_1(5721)^{0,+}$ and $B_2^*(5747)^{0,+}$ were observed by the D0 experiment [2], and were confirmed by the CDF experiment one year later [3]. Their strange analogues, $B_{s1}(5830)$ and $B_{s2}^*(5840)$, as the first orbitally excited B_s mesons, were also reported by the CDF Collaboration in 2007 [4]. The $B_{s1}(5830)$ and $B_{s2}^*(5840)$ were confirmed by the D0 and LHCb experiments [5,6]. In 2013, two higher resonances $B(5970)^{0,+}$ were observed in the $B\pi$ final states by the CDF Collaboration [7]. In 2015, four higher resonances $B_J(5840)^{0,+}$ and $B_J(5960)^{0,+}$ were observed in the $B\pi$ final states by the LHCb Collaboration when they carried out precise measurements of the properties of the $B_1(5721)^{0,+}$ and $B_2^*(5747)^{0,+}$ states [8]. The properties of the $B_J(5960)^{0,+}$ states are consistent with those of $B(5970)^{0,+}$ obtained by the CDF Collaboration. Recently, the LHCb Collaboration observed two structures $B_{sJ}(6064)$ and $B_{sJ}(6114)$ in the B^+K^- mass spectrum [9]. More experimental information about the excited bottom and bottom-strange mesons is collected in Table I. More and more excited bottom and bottom-strange mesons are expected to be observed in future LHCb experiments due to its huge production cross sections of beauty, together with a good reconstruction efficiency, versatile trigger scheme and an excellent momentum and mass resolution [10].

In theory, many theoretical studies of the masses [11–29], strong decays [24–43], radiative decays [23,26–29,42–44], and weak decays [23,45,46] for the excited bottom and bottom-strange meson states have been carried out with different methods. For the well established states $B_1(5721)$, $B_2^*(5747)$, $B_{s1}(5830)$ and $B_{s2}^*(5840)$, there are no puzzles to classify them as the first orbital excitations (i.e., the $1P$-wave states) of quark models. While for the newly observed resonances/structures $B_J(5840)^{0,+}$, $B(5970)^{0,+}$, $B_{sJ}(6064)$, and $B_{sJ}(6114)$, although they are good candidates of the $2S$ and $1D$-wave states according to the mass spectrum predictions in various quark models, their quark model classification is not clear. There are some theoretical

*zhongxh@hunnu.edu.cn

TABLE I. Summary of the experimental information for the excited B- and B_s-meson states. The date for the $B_1(5721)^{+,0}$, $B_2(5747)^{+,0}$, $B_{s1}(5830)^0$, and $B_{s2}(5840)^0$ resonances are adopted the average values of the Review of Particle Physics (RPP) of Particle Data Group (PDG) [1]. The N and UN stand for the natural spin parity $P=(-1)^J$ and unnatural spin parity $P=-(-1)^J$.

	Resonance	J^P	Mass (MeV)	Width (MeV)	Observed channel	Experiment
	$B_1(5721)^0$	1^+	5726.1 ± 1.3	27.5 ± 3.4	$B^{*+}\pi^-$	D0 [2], CDF [3], LHCb [8]
	$B_1(5721)^+$	1^+	$5725.9^{+2.5}_{-2.7}$	31 ± 6	$B^{*0}\pi^+$	D0 [2], CDF [3], LHCb [8]
	$B_2(5747)^0$	2^+	5739.5 ± 0.7	24.2 ± 1.7	$B^+\pi^-$,$B^{*+}\pi^-$	D0 [2], CDF [3], LHCb [8]
	$B_2(5747)^+$	2^+	5737.2 ± 0.7	20 ± 5	$B^+\pi^-$,$B^{*+}\pi^-$	D0 [2], CDF [3], LHCb [8]
	$B_J(5970)^+$	?	5961 ± 17	$60^{+30}_{-20} \pm 40$	$B^0\pi^+$ [or $B^{*0}\pi^+$]	CDF [7]
	$B_J(5970)^0$	?	5978 ± 17	$70^{+30}_{-20} \pm 30$	$B^+\pi^-$ [or $B^{*+}\pi^-$]	CDF [7]
Case A	$B_J(5960)^+$	UN	5964.9 ± 6.8	63.0 ± 31.7	$B^{*0}\pi^+$	LHCb [8]
	$B_J(5960)^0$	UN	5969.2 ± 8.2	82.3 ± 17.1	$B^{*+}\pi^-$	LHCb [8]
	$B_J(5840)^+$	UN	5850.3 ± 26.6	224.4 ± 103.7	$B^{*0}\pi^+$	LHCb [8]
	$B_J(5840)^0$	UN	5862.9 ± 11.9	127.4 ± 50.9	$B^{*+}\pi^-$	LHCb [8]
Case B	$B_J(5960)^+$	UN	6010.6 ± 7.1	61.4 ± 31.7	$B^{*0}\pi^+$	LHCb [8]
	$B_J(5960)^0$	UN	6015.9 ± 9.2	81.6 ± 19.3	$B^{*+}\pi^-$	LHCb [8]
	$B_J(5840)^+$	N	5874.5 ± 39.6	214.6 ± 106.5	$B^{*0}\pi^+$, $B^0\pi^+$?	LHCb [8]
	$B_J(5840)^0$	N	5889.7 ± 29.1	107.0 ± 53.8	$B^{*+}\pi^-$, $B^+\pi^-$?	LHCb [8]
Case C	$B_J(5960)^+$	N	5966.4 ± 7.2	60.8 ± 31.2	$B^{*0}\pi^+$, $B^0\pi^+$?	LHCb [8]
	$B_J(5960)^0$	N	5993.6 ± 11.7	55.9 ± 16.0	$B^{*+}\pi^-$, $B^+\pi^-$?	LHCb [8]
	$B_J(5840)^+$	UN	5889.3 ± 29.3	229.3 ± 104.7	$B^{*0}\pi^+$	LHCb [8]
	$B_J(5840)^0$	UN	5907.8 ± 13.0	119.4 ± 51.4	$B^{*+}\pi^-$	LHCb [8]
	$B_{s1}(5830)^0$	1^+	5828.70 ± 0.20	$0.5 \pm 0.3 \pm 0.3$	$B^{*+}K^-$, $B^{*0}K^0$	CDF [4], D0 [6], LHCb [5]
	$B_{s2}(5840)^0$	2^+	5839.86 ± 0.12	1.49 ± 0.27	B^*K, BK	CDF [4], D0 [6], LHCb [5]
	$B_{sJ}(6064)^0$	?	6063.5 ± 2.0	$26 \pm 4 \pm 4$	B^+K^-	LHCb [9]
	[or $B_{sJ}(6109)^0$]	?	[or 6108.8 ± 1.8]	[or $22 \pm 5 \pm 4$]	[or $B^{*+}K^-$]	LHCb [9]
	$B_{sJ}(6114)^0$	?	6114 ± 8	$66 \pm 18 \pm 21$	B^+K^-	LHCb [9]
	[or $B_{sJ}(6158)^0$]	?	[or 6158 ± 9]	[or $72 \pm 18 \pm 25$]	[or $B^{*+}K^-$]	LHCb [9]

interpretations of the newly observed $B_J(5840)$ and $B_J(5970)$ based on the predicted masses and strong decay properties, since they have been reported by the CDF and LHCb experiments. In the literature, the $B_J(5840)$ resonance is explained with the $B(2^1S_0)$ [27,28,39], the $B(2^3S_1)$ [31], or the $B(1^3D_1)$ state [40]. While for the resonance $B_J(5970)$, there are interpretations with the radially excited state $B(2^3S_1)$ [15,25,39], or with the second orbitally excited B-meson states [29] either $B(1^3D_3)$ [27,31] or $B(1^3D_1)$ [28]. It should be mentioned that in Ref. [47], our group assigned the $B_J(5970)$ resonance to be the $B(1^3D_3)$ state by analyzing the strong decay properties within a chiral quark model. Based on this assignment, the authors further predicted that as the partner of $B_J(5970)$, the mass and width of the $B_s(1^3D_3)$ state might be $M \simeq 6.07$ GeV and $\Gamma \simeq 30$ MeV, respectively, which are also in agreement with those predictions in Refs. [27,28]. If assigning the $B_{sJ}(6064)$ to be the $B_s(1^3D_3)$ state, both the measured mass and width are consistent with quark model predictions. It should be mentioned that there are no discussions about the recently observed structures $B_{sJ}(6064)$ and $B_{sJ}(6114)$ in the literature. More information about the status of the bottom and bottom-strange meson study can be found in the recent review work [48].

The experimental progress provides us good opportunities to establish an abundant B and B_s-meson spectrum up to the second orbital ($L=2$) excitations. In this work we deepen our study by carrying out a combined analysis of the masses and decay properties of the B and B_s-meson states up to the $L=2$ excitations. First, we calculate the mass spectrum of B and B_s mesons within a nonrelativistic potential model. With this model the masses for the observed B and B_s-meson states can be described successfully. Then, with the available wave functions from the potential model, we calculate the Okubo-Zweig-Iizuka (OZI)-allowed two-body strong decays of the excited B and B_s mesons with a chiral quark model [49–52]. This model has been successfully applied to describe the strong decays of the heavy-light mesons and baryons [24,47,53–64]. To provide more knowledge for the excited B and B_s meson states, we also evaluate their electromagnetic (EM) transitions within a nonrelativistic constituent quark model [50–52,65–71]. This model has also been successfully applied to describe the radiative decays of baryon states [60–64,72,73] and meson systems [74–78]. Based on our good descriptions of the mass and decay properties for the low-lying well-established states $B_1(5721)^{0,+}$, $B_2^*(5747)^{0,+}$, $B_{s1}(5830)$

and $B^*_{s2}(5840)$, we give our quark model classifications of the high mass resonances/structures $B_J(5840)^{0,+}$, $B(5970)^{0,+}$, $B_{sJ}(6064)$, and $B_{sJ}(6114)$. Finally, according to our assignments for the newly observed resonances, we attempt to predict the properties of the missing resonances, which may be useful for future investigations in experiments.

This paper is organized as follows. In Sec. II, the mass spectrum is calculated within a nonrelativistic linear potential model. In Sec. III, a brief review of the chiral quark model is given. The numerical results are presented and discussed in Sec. IV. Finally, a summary is given in Sec. V.

II. MASS SPECTRUM

To describe the bottom and bottom-strange meson spectra, we adopt a nonrelativistic linear potential model. In this model, the effective potential is adopted as [79–82]

$$V(r) = V_0(r) + V_{sd}(r), \tag{1}$$

where

$$V_0(r) = -\frac{4}{3}\frac{\alpha_s}{r} + br + C_0 \tag{2}$$

includes the standard color Coulomb interaction and linear confinement, and zero point energy C_0. The spin-dependent part $V_{sd}(r)$ can be expressed as [81–83]

$$V_{sd}(r) = H_{SS} + H_T + H_{\rm LS}, \tag{3}$$

where

$$H_{SS} = \frac{32\pi\alpha_s}{9m_q m_{\bar{q}}}\tilde{\delta}_\sigma(r)\mathbf{S}_q\cdot\mathbf{S}_{\bar{q}} \tag{4}$$

is the spin-spin contact hyperfine potential. Here, we take $\tilde{\delta}_\sigma(r) = (\sigma/\sqrt{\pi})^3 e^{-\sigma^2 r^2}$ as suggested in Ref. [79]. The tensor potential H_T is adopted as

$$H_T = \frac{4}{3}\frac{\alpha_s}{m_q m_{\bar{q}}}\frac{1}{r^3}S_T, \tag{5}$$

with $S_T = \frac{3\mathbf{S}_q\cdot\mathbf{r}\mathbf{S}_{\bar{q}}\cdot\mathbf{r}}{r^2} - \mathbf{S}_q\cdot\mathbf{S}_{\bar{q}}$.

The spin-orbit interaction $H_{\rm LS}$ can be decomposed into symmetric part $H_{\rm sym}$ and antisymmetric part $H_{\rm anti}$:

$$H_{\rm LS} = H_{\rm sym} + H_{\rm anti}, \tag{6}$$

with

$$H_{\rm sym} = \frac{\mathbf{S}_+\cdot\mathbf{L}}{2}\left[\left(\frac{1}{2m_{\bar{q}}^2}+\frac{1}{2m_q^2}\right)\left(\frac{4}{3}\frac{\alpha_s}{r^3}-\frac{b}{r}\right)+\frac{8\alpha_s}{3m_q m_{\bar{q}} r^3}\right], \tag{7}$$

$$H_{\rm anti} = \frac{\mathbf{S}_-\cdot\mathbf{L}}{2}\left(\frac{1}{2m_{\bar{q}}^2}-\frac{1}{2m_q^2}\right)\left(\frac{4}{3}\frac{\alpha_s}{r^3}-\frac{b}{r}\right). \tag{8}$$

In these equations, $\mathbf{L}$ is the relative orbital angular momentum of the $q\bar{q}$ system; $\mathbf{S}_q$ and $\mathbf{S}_{\bar{q}}$ are the spins of the quark q and antiquark $\bar{q}$, respectively, and $\mathbf{S}_\pm \equiv \mathbf{S}_q \pm \mathbf{S}_{\bar{q}}$; m_q and $m_{\bar{q}}$ are the masses of quark q and antiquark $\bar{q}$, respectively; α_s is the running coupling constant of QCD; and r is the distance between the quark q and antiquark $\bar{q}$. The six parameters in the above potentials (α_s, b, σ, m_q, $m_{\bar{q}}$, C_0) are determined by fitting the mass spectrum.

It should be emphasized that when $m_q \neq m_{\bar{q}}$, the antisymmetric part of the spin-orbit potential, $H_{\rm anti}$, can cause a configuration mixing between spin triplet n^3L_J and spin singlet n^1L_J. Thus, the physical states nL_J and nL'_J are expressed as

$$\begin{pmatrix} nL_J \\ nL'_J \end{pmatrix} = \begin{pmatrix} \cos\theta_{nL} & \sin\theta_{nL} \\ -\sin\theta_{nL} & \cos\theta_{nL} \end{pmatrix}\begin{pmatrix} n^1L_J \\ n^3L_J \end{pmatrix}. \tag{9}$$

where $J = L = 1, 2, 3\cdots$, and the θ_{nL} is the mixing angle. In this work nL'_J corresponds to the higher mass mixed state as often adopted in the literature.

In this work, we solve the radial Schrödinger equation by using the three-point difference central method [84] from central ($r = 0$) toward outside ($r \to \infty$) point by point. This method was successfully to deal with the spectroscopies of $c\bar{c}$, $b\bar{b}$, $b\bar{c}$ and $s\bar{s}$ [76–78,85,86]. To overcome the singular behavior of $1/r^3$ in the spin-dependent potentials, following the method of our previous works [76–78,85,86], we introduce a cutoff distance r_c in the calculation. Within a small range $r \in (0, r_c)$, we let $1/r^3 = 1/r_c^3$. By introducing the cutoff distance r_c, we can nonperturbatively include the corrections from these spin-dependent potentials containing $1/r^3$ to both the mass and wave function of a meson state, which are crucial for our predicting the decay properties.

The model parameters adopted in this work are listed in Table II. To be consistent with our previous study [64,78,85,86], the bottom quark mass m_b, the light up or down quark mass $m_{u/d}$, the strange quark mass m_s are taken from the determinations, i.e., $m_b = 4.852$ GeV, $m_{u/d} = 0.45$ GeV, $m_s = 0.60$ GeV. The other four parameters (α_s, b, σ, C_0) for the bottom meson sector, they are determined by fitting the masses of the well-established states $B(5279)$, $B^*(5325)$, $B_1(5721)$ and $B_2^*(5747)$, while for the bottom-strange meson sector, they are determined by fitting the masses of the well-established states $B_s(5367)$, $B_s^*(5415)$, $B_{s1}(5830)$ and $B_{s2}^*(5840)$. It should

TABLE II. The parameters of the nonrelativistic potential model.

	B	B_s
m_b (GeV)	4.852	4.852
$m_{u,d}$ (GeV)	0.450	...
m_s (GeV)	...	0.600
α	0.564	0.550
σ (GeV)	0.98	1.06
b (GeV^2)	0.120	0.120
C_0 (GeV)	−0.2537	−0.2318
r_c (fm)	0.337	0.292

be pointed out that the zero-point-energy parameter C_0 is taken to be zero for the $c\bar{c}$, $b\bar{b}$, $b\bar{c}$ heavy quarkonium systems in the literature [76–78,85]. For these heavy quarkonium systems, the zero point energy can be absorbed into the constituent quark masses because it only affects the heavy quark masses slightly. However, if the zero point energy is absorbed into the meson systems containing light quarks, it can significantly change the light constituent quark masses, which play an important role in the spin-dependent potentials. Thus, to obtain a good description of both the masses and the hyperfine/fine splittings for the meson systems containing light quarks, a zero-point-energy parameter C_0 is usually adopted in the calculations.

Finally, we need determine the cutoff distance r_c in our calculations. It is found that the masses of the 1^3P_0 states are more sensitive to the cutoff distance r_c. The reason is that the singular terms of $1/r^3$ in the spin-dependent potentials have more effects on the mass of the 1^3P_0 state due to its relatively larger factors of $\langle \mathbf{S}_+ \cdot \mathbf{L} \rangle$ and $\langle S_T \rangle$ than the other excited meson states. Thus, in the present work, we determine the r_c by fitting the masses of the $B(1^3P_0)$ and $B_s(1^3P_0)$ states. Note that when the other parameters are well determined, the masses of these 1^3P_0 states can be reliably worked out with the perturbation method without introducing the cutoff distance r_c, although the wave functions obtain no corrections from the spin-dependent potentials containing $1/r^3$. To calculate the masses of the $B(1^3P_0)$ and $B_s(1^3P_0)$ states with the perturbation method, we let $H = H_0 + H'$, where H_0 is the main part of the Hamiltonian without singular $1/r^3$ term contributions, i.e.,

$$H_0 = \frac{P^2}{2\mu} + V_0(r) + \frac{32\pi\alpha_s}{9m_q m_{\bar{q}}}\tilde{\delta}_\sigma(r)\langle \mathbf{S}_q \cdot \mathbf{S}_{\bar{q}} \rangle + \frac{\langle \mathbf{S}_+ \cdot \mathbf{L} \rangle}{2}\left[\left(\frac{1}{2m_{\bar{q}}^2} + \frac{1}{2m_q^2}\right)\left(-\frac{b}{r}\right)\right], \quad (10)$$

where $\frac{P^2}{2\mu}$ is the kinetic energy term with a reduced mass $\mu = m_q m_{\bar{q}}/(m_q + m_{\bar{q}})$; while H' is the perturbation part containing $1/r^3$ terms, i.e.,

$$H' = \frac{\langle \mathbf{S}_+ \cdot \mathbf{L} \rangle}{2}\left[\left(\frac{1}{2m_{\bar{q}}^2} + \frac{1}{2m_q^2}\right)\left(\frac{4}{3}\frac{\alpha_s}{r^3}\right) + \frac{8\alpha_s}{3m_q m_{\bar{q}} r^3}\right] + \frac{4}{3}\frac{\alpha_s}{m_q m_{\bar{q}}}\frac{1}{r^3}\langle S_T \rangle. \quad (11)$$

For a 1^3P_0 state, one can easily obtain the matrix elements $\langle \mathbf{S}_q \cdot \mathbf{S}_{\bar{q}} \rangle = 1/4$, $\langle \mathbf{S}_+ \cdot \mathbf{L} \rangle = -2$, and $\langle S_T \rangle = -1$ by using the relations $\langle \mathbf{S}_q \cdot \mathbf{S}_{\bar{q}} \rangle = S(S+1)/2 - 3/4$, $\langle \mathbf{S}_+ \cdot \mathbf{L} \rangle = [J(J+1) - L(L+1) - S(S+1)]/2$, and $\langle S_T \rangle = -[6\langle \mathbf{S}_+ \cdot \mathbf{L} \rangle^2 + 3\langle \mathbf{S}_+ \cdot \mathbf{L} \rangle - 2\mathbf{L}^2\mathbf{S}_+^2]/[2(2L-1)(2L+3)]$. By solving the radial Schrödinger equation of $H_0\psi^{(0)}(r) = E_0\psi^{(0)}(r)$ with the three-point difference central method, we work out the eigenenergies $E_0 = 508, 415$ MeV for the $B(1^3P_0)$ and $B_s(1^3P_0)$ states as well as their zero order radial wave functions $\psi^{(0)}(r)$. Using these zero order wave functions, we further work out the perturbation energies $\langle \psi^{(0)}(r)|H'|\psi^{(0)}(r)\rangle = -88, -79$ MeV for the $B(1^3P_0)$ and $B_s(1^3P_0)$ states, respectively. Finally, with the relation $M = m_q + m_{\bar{q}} + E_0 + \langle \psi^{(0)}(r)|H'|\psi^{(0)}(r)\rangle$ we predict the masses 5722 and 5788 MeV for $B(1^3P_0)$ and $B_s(1^3P_0)$, respectively. These masses calculated with the perturbation method are in good agreement with the predictions in the literature [12–14,24,28]. Within a small range $r \in (0, r_c)$, letting $1/r^3 = 1/r_c^3$ in the perturbation Hamiltonian H', we solve the radial Schrödinger equation $(H_0 + H')\psi(r) = E\psi(r)$ with the three-point difference central method again. By reproducing the masses 5722 and 5788 MeV of the $B(1^3P_0)$ and $B_s(1^3P_0)$ states obtained with the perturbation method, we determine the cutoff distance parameters $r_c = 0.337$ and 0.292 fm for the B and B_s mass spectra, respectively. The corrections of the perturbation part H' to the radial wave function $\psi(r)$ can be conveniently included by introducing the cutoff distance r_c. As an

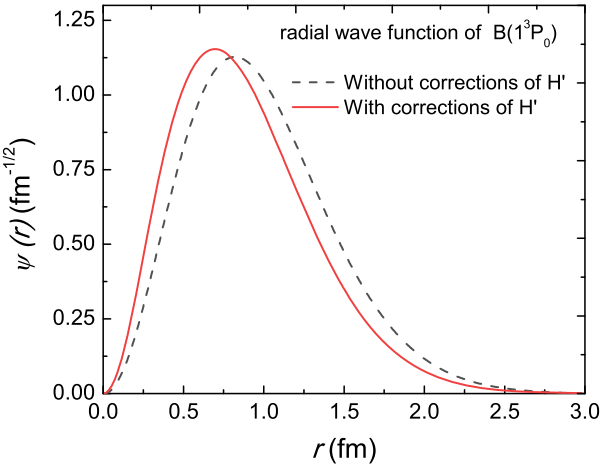

FIG. 1. The radial wave function $\psi(r)$ of the $B(1^3P_0)$ state. The solid and dashed lines stand for the wave functions with and without corrections from the perturbation term H' containing $1/r^3$, respectively.

TABLE III. The predicted bottom meson masses (MeV) compared with the data and some other model predictions. The mixing angle of $1^3P_1 - 1^1P_1$ and $1^3D_2 - 1^1D_2$ obtained in present work are $\theta_{1P} = -35.2°$, and $\theta_{1D} = -39.5°$. In the table, $\beta^{NR}_{\rm eff}$ and $\beta^{R}_{\rm eff}$ stand for the effective harmonic oscillator parameters (GeV) of our nonrelativistic quark model calculations and those with the relativized quark model calculations [26], respectively, while $\beta^{C}_{\rm eff}$ stands for our results including relativistic corrections of the length contraction effects.

State	J^P	$\beta^{NR}_{\rm eff}$	$\beta^{C}_{\rm eff}$	$\beta^{R}_{\rm eff}$ [26]	Ours	KDR [13]	EFG [14]	LPW [27]	LL [15]	GI [26]	AMS [28]	PE [24]	Exp. [1]
$B(1^1S_0)$	0^-	0.444	0.628	0.580	5279(fitted)	5287	5280	5280	5273	5312	5268	5279	5280
$B(1^3S_1)$	1^-	0.418	0.575	0.542	5325(fitted)	5323	5326	5329	5329	5371	5329	5324	5325
$B(1^3P_0)$	0^+	0.367	0.525	0.536	5722	5730	5749	5683	5776	5756	5704	5706	···
$B(1P_1)$	1^+	0.348	0.487	0.511	5716	5733	5723	5729	5719	5784	5739	5700	5698
$B(1P_1')$	1^+	0.348	0.487	0.499	5753(fitted)	5752	5744	5754	5837	5777	5755	5742	5726
$B(1^3P_2)$	2^+	0.334	0.460	0.472	5727(fitted)	5740	5741	5768	5739	5797	5769	5714	5740
$B(2^1S_0)$	0^-	0.327	0.472	0.477	5876	5926	5890	5910	5957	5904	5877	5886	5863
$B(2^3S_1)$	1^-	0.320	0.458	0.468	5899	5947	5906	5939	5997	5933	5905	5920	···
$B(1^3D_1)$	1^-	0.316	0.453	0.488	6056	6016	6119	6095	6143	6110	6022	6025	···
$B(1D_2)$	2^-	0.312	0.445	0.463	5973	6031	6103	6004	5993	6095	6026	5985	···
$B(1D_2')$	2^-	0.312	0.445	0.469	6067	6065	6121	6113	6165	6124	6031	6037	···
$B(1^3D_3)$	3^-	0.312	0.445	0.444	5979	6016	6091	6014	6004	6106	6031	5993	5971

TABLE IV. The predicted bottom-strange meson masses (MeV) compared with the data and some other model predictions. The mixing angle of $1^3P_1 - 1^1P_1$ and $1^3D_2 - 1^1D_2$ obtained in present work are $\theta_{1P} = -39.6°$, and $\theta_{1D} = -39.9°$. In the table, $\beta^{NR}_{\rm eff}$ and $\beta^{R}_{\rm eff}$ stand for the effective harmonic oscillator parameters (GeV) obtained from our nonrelativistic quark model calculations and those with the relativized quark model calculations [26], respectively, while $\beta^{C}_{\rm eff}$ stands for our results including relativistic corrections of the length contraction effects.

State	J^P	$\beta^{NR}_{\rm eff}$	$\beta^{C}_{\rm eff}$	$\beta^{R}_{\rm eff}$ [26]	Ours	KDR [13]	EFG [14]	ZVR [12]	LPW [27]	AMS [28]	GI [26]	PE [24]	Exp.
$B_s(1^1S_0)$	0^-	0.507	0.681	0.636	5367(fitted)	5367	5372	5370	5362	5377	5394	5373	5367 [1]
$B_s(1^3S_1)$	1^-	0.475	0.621	0.595	5415(fitted)	5413	5414	5430	5413	5422	5450	5421	5416 [1]
$B_s(2^1S_0)$	0^-	0.363	0.490	0.508	5944	6003	5976	5930	5977	5929	5984	5985	···
$B_s(2^3S_1)$	1^-	0.356	0.465	0.497	5966	6029	5992	5970	6003	5949	6012	6019	···
$B_s(1^3P_0)$	0^+	0.408	0.549	0.563	5788	5812	5833	5750	5756	5770	5831	5804	···
$B_s(1P_1)$	1^+	0.387	0.509	0.538	5810	5828	5831	5790	5801	5801	5857	5805	···
$B_s(1P_1')$	1^+	0.387	0.509	0.528	5821(fitted)	5842	5865	5800	5836	5803	5861	5842	5829 [1]
$B_s(1^3P_2)$	2^+	0.369	0.477	0.504	5821(fitted)	5840	5842	5820	5851	5822	5876	5820	5840 [1]
$B_s(1^3D_1)$	1^-	0.351	0.472	0.504	6101	6119	6209	6070	6142	6057	6182	6127	6114 [9]
$B_s(1D_2)$	2^-	0.344	0.459	0.487	6061	6128	6189	6070	6087	6059	6169	6095	···
$B_s(1D_2')$	2^-	0.344	0.459	0.482	6113	6157	6218	6080	6159	6064	6196	6140	6109 [9]
$B_s(1^3D_3)$	3^-	0.340	0.451	0.467	6067	6172	6191	6080	6096	6063	6179	6103	6064 [9]

example, in Fig. 1 we plot the radial wave functions of the $B(1^3P_0)$ state with and without the corrections from the perturbation part H' containing $1/r^3$. It is seen that the perturbation term H' has an obvious correction to the radial wave function.

With the determined model parameters listed in Table II, by solving the radial Schrödinger equation we obtain the masses of the bottom and bottom-strange meson states, which have been listed in Tables III and IV, respectively. For comparison, some other model predictions in Refs. [12–15,24,26–28] and the data from the Review of Particle Physics (RPP) of Particle Data Group (PDG) [1] are listed in the same table as well. Furthermore, for a clarity, the spectra are also shown in Fig. 2. It is shown that the $B_J(5970)$ resonance and the structures $B_{sJ}(6064)$ and $B_{sJ}(6114)$ newly observed at LHCb can be explained as the $1D$-wave states from the point of view of the mass, while the $B_J(5840)$ may be a good candidate of the $2S$-wave state.

III. STRONG AND RADIATIVE DECAYS

A. Models

We calculate the strong decays of the bottom and bottom-strange mesons with the chiral quark model [49–52]. In this model, the light pseudoscalar mesons, i.e,. π, K,

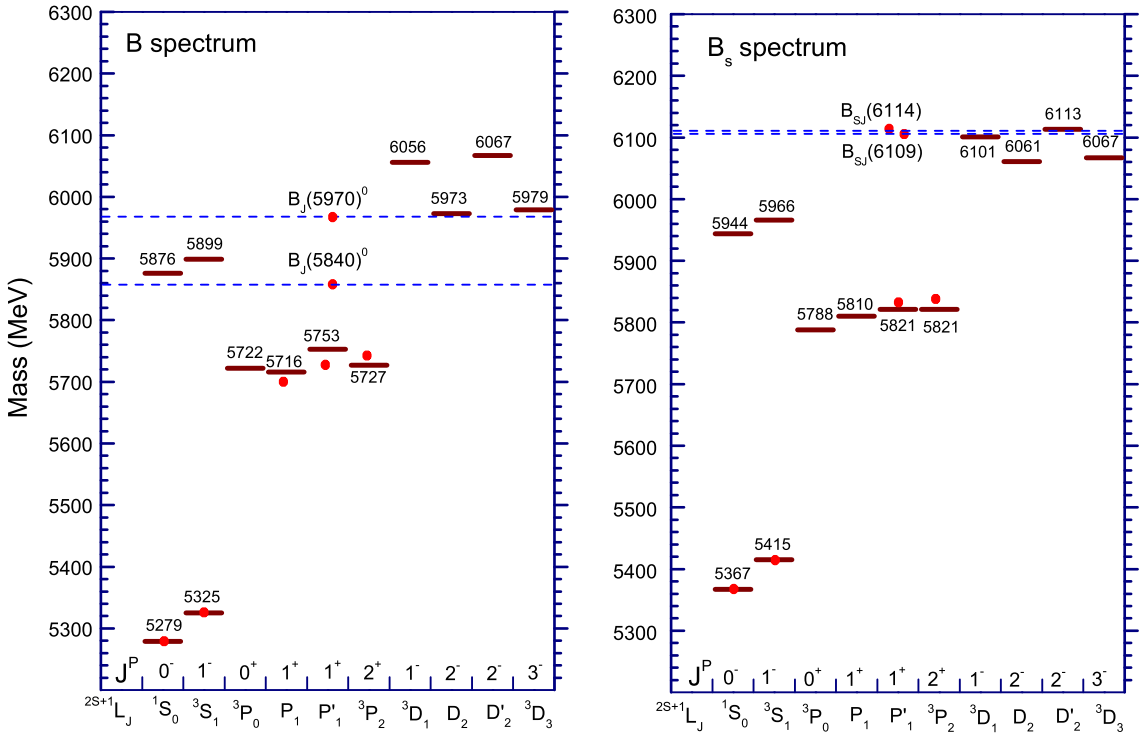

FIG. 2. The predicted mass spectra of B and B_s mesons. The solid circles stand for the measured masses obtained from the Particle Data Group [1] and the recent LHCb measurements [9].

and η, are treated as fundamental states. The low energy quark-pseudoscalar-meson and quark-vector-meson interactions in the SU(3) flavor basis are described by the effective Lagrangian

$$H_m = \sum_j \frac{1}{f_m} \bar{\psi}_j \gamma_\mu \gamma_5 \psi_j \vec{\tau} \cdot \partial^\mu \vec{\phi}_m, \tag{12}$$

where ψ_j represents the jth quark field in the hadron, ϕ_m is the pseudoscalar meson field, f_m is the pseudoscalar meson decay constant. The nonrelativistic form of Eq. (12) is given by [50–52]

$$H_m = \sum_j [A\boldsymbol{\sigma}_j \cdot \mathbf{q} + h\boldsymbol{\sigma}_j \cdot \mathbf{p}_j] I_j \varphi_m, \tag{13}$$

in the center-of-mass system of the initial meson, where we have defined $A \equiv -(1 + \frac{\omega_m}{E_f + M_f})$ and $h \equiv \frac{\omega_m}{2\mu_q}$. In Eq. (13), $\mathbf{q}$ and ω_m are the three-vector momentum and energy of the final-state light meson, respectively; $\mathbf{p}_j$ is the internal momentum operator of the jth quark in the heavy-light meson rest frame; $\boldsymbol{\sigma}_j$ is the spin operator corresponding to the jth quark of the heavy-light system; and μ_q is a reduced mass given by $1/\mu_q = 1/m_j + 1/m'_j$ with m_j and m'_j for the masses of the jth quark in the initial and final mesons, respectively. The plane wave part of the emitted light meson is $\varphi_m = e^{-i\mathbf{q}\cdot\mathbf{r}_j}$, and I_j is the flavor operator defined for the transitions in the SU(3) flavor space. The chiral quark model has been successfully applied to describe the strong decays of the heavy-light mesons and baryons [24,47,53–59]. The details of this model can be found in Refs. [55,56]. It should be mentioned that the chiral quark model is similar to the pseudoscalar emission model in the literature [11,87,88]. The nonrelativistic form of quark-pseudoscalar-meson interactions expressed in Eq. (13) is similar to that of the pseudoscalar emission model, except that the factors $A \equiv -(1 + \frac{\omega_m}{E_f + M_f})$ and $h \equiv \frac{\omega_m}{2\mu_q}$ in this work have an explicit dependence on the energies of final hadrons.

Meanwhile, to treat the radiative decay of a hadron we apply the constituent quark model [50–52,65–71]. In this model, the quark-photon EM coupling at the tree level is adopted as

$$H_e = -\sum_j e_j \bar{\psi}_j \gamma_\mu^j A^\mu(\mathbf{k}, \mathbf{r}_j) \psi_j, \tag{14}$$

where A^μ represents the photon field with three-momentum $\mathbf{k}$. e_j and $\mathbf{r}_j$ stand for the charge and coordinate of the constituent quark ψ_j, respectively. In the initial-hadron-rest system, including the effects of the binding potential between quarks, the nonrelativistic form of the quark-photon EM coupling can be written as [50–52,65,68–71]

$$H_e^{nr} = \sum_j \left[e_j \mathbf{r}_j \cdot \boldsymbol{\epsilon} - \frac{e_j}{2m_j} \boldsymbol{\sigma}_j \cdot (\boldsymbol{\epsilon} \times \hat{\mathbf{k}}) \right] \varphi_\gamma, \quad (15)$$

where $\boldsymbol{\sigma}_j$ stand for the Pauli spin vector for the jth quark. The vector $\boldsymbol{\epsilon}$ is the polarization vector of the photon. The plane wave part of the emitted light meson is $\varphi_\gamma = e^{-i\mathbf{k}\cdot\mathbf{r}_j}$. The first and second terms in Eq. (15) are responsible for the electric and magnetic transitions, respectively. The second term in Eq. (15) is the same as that used in Refs. [11,87–90], while the first term in Eq. (15) is different from $(1/m_j)\mathbf{p}_j \cdot \boldsymbol{\epsilon}$ of these works due to the binding potential effects are included [65]. This model has been successfully applied to describe the radiative decays of baryon states [60–64,72,73] and meson systems [74–78].

For a strong decay process, the partial decay width is calculated with [55,56]

$$\Gamma_m = \left(\frac{\delta}{f_m}\right)^2 \frac{(E_f + M_f)|\mathbf{q}|}{4\pi M_i (2J_i + 1)} \sum_{J_{fz}, J_{iz}} |\mathcal{M}_{J_{fz},J_{iz}}|^2, \quad (16)$$

while for a radiative decay process, the partial decay width is calculated with [76,77]

$$\Gamma_\gamma = \frac{|\mathbf{k}|^2}{\pi} \frac{2}{2J_i + 1} \frac{M_f}{M_i} \sum_{J_{fz}, J_{iz}} |\mathcal{A}_{J_{fz},J_{iz}}|^2, \quad (17)$$

where $\mathcal{M}_{J_{fz},J_{iz}}$ and $\mathcal{A}_{J_{fz},J_{iz}}$ correspond to the strong and radiative transition amplitudes, respectively. The quantum numbers J_{iz} and J_{fz} stand for the third components of the total angular momenta of the initial and final hadron states, respectively. δ as a global parameter accounts for the strength of the quark-meson couplings. It has been determined in our previous study of the strong decays of the charmed baryons and heavy-light mesons [55,56]. Here, we fix its value the same as that in Refs. [55,56], i.e., $\delta = 0.557$.

B. Parameters

In the calculation, the constituent quark masses for the u, d, and s quarks are taken with $m_u = m_d = 450$ MeV and $m_s = 600$ MeV to be consistent with the spectrum study in Sec. II. The decay constants for π, K and η mesons are taken as $f_\pi = 132$ MeV, $f_K = f_\eta = 160$ MeV, respectively. The masses of the well-established hadrons involving in the calculations are adopted from the PDG [1]. The masses of the missing B- and B_s-meson states are adopted our determinations by solving the Schröinger equation in Sec. II.

It should be mentioned that, we do not directly adopt the numerical wave functions of B- and B_s-meson states calculated by solving the Schröinger equation. For simplicity, we first fit them with a simple harmonic oscillator wave function by reproducing the root-mean-square radius $\sqrt{\langle r^2 \rangle}$. The obtained effective harmonic oscillator parameters $\beta_{\rm eff}$ for the meson states are listed in Tab. III and Tab. IV. It is found that the effective harmonic oscillator parameters $\beta_{\rm eff}^{NR}$ obtained from our nonrelativistic quark model calculations are obviously smaller than the parameters $\beta_{\rm eff}^{R}$ obtained from the relativized quark models [26]. It indicates that the relativistic effects of the length contraction on the wave function may be important. To take into account the relativistic effects, as that suggested in Ref. [91] we introduce the Lorentz boost factor γ in the spatial wave function, i.e.,

$$\psi_{nlm}(\mathbf{r}) \to \psi_{nlm}(\gamma \mathbf{r}), \quad (18)$$

where $\gamma = M_q/E_q$. M_q and E_q correspond to the effective mass and energy of the light quark, respectively. According to Ref. [92], the effective mass M_q can be estimated by $M_q = \sqrt{\langle p^2 \rangle + m_q^2}$, while the energy E_q is estimated by $E_q = \langle p \rangle^2/(2M_q) + M_q$. To realize this transformation, we only need replace $\beta_{\rm eff}^{NR}$ in the harmonic oscillator wave function with $\beta_{\rm eff}^{C} = \gamma \beta_{\rm eff}^{NR}$. The effective harmonic oscillator parameters $\beta_{\rm eff}^{C}$ including relativistic corrections of the length contraction are given in Tables III and IV as well. It is found that the $\beta_{\rm eff}^{C}$ values are comparable with those obtained with the relativized quark models [26]. In Refs. [47,55], the strong decays of the heavy-light meson states are studied with the chiral quark model by using the simple harmonic oscillator wave functions with fixed harmonic oscillator parameters $\beta = 468$, 466 MeV for the B and B_s spectra, respectively, which are close to the parameters $\beta_{\rm eff}^{C}$ determined for the $1P$-, $1D$- and $2S$-wave states in present work. The parameters $\beta_{\rm eff}^{C}$ of the ground states 1^1S_0 and 1^3S_1 are notably lager than that of the excited states, this effect is mainly caused by the strong color Coulomb interaction at the small distance r between two quarks.

The effective parameters $\beta_{\rm eff}^{C}$ of the ground states $B(1^1S_0)$ and $B^*(1^3S_1)$ are crucial for understanding the decay properties of the excited B and B_s states because all of the excited states should decay into these ground states. Considering the uncertainty of the parameters $\beta_{\rm eff}^{C}$ of the ground states $B(1^1S_0)$ and $B^*(1^3S_1)$, we properly adjust their $\beta_{\rm eff}^{C}$ parameters to more reasonably describe the strong decay properties of the well established $1P$-wave states $B_2^*(5747)^0$ and $B_{s2}^*(5840)$. In this work, we determine them to be $\beta_{B(1^1S_0)} = 0.537$ GeV and $\beta_{B^*(1^3S_1)} = 0.510$ GeV for $B(1^1S_0)$ and $B^*(1^3S_1)$, respectively. There is about a 10% correction to the effective parameters $\beta_{\rm eff}^{C}$.

With above parameters, our calculated decay properties for the $1P$-, $2S$-, and $1D$-wave states are listed in Tables V–VII, respectively. From Table V, it is found that the decay properties of the well-established $1P$-wave state can be successfully described.

TABLE V. Partial and total decay widths (MeV) for $1P$-wave bottom and bottom-strange mesons compared with the data and some recent model predictions. It should be mentioned that some masses for the initial states adopted in the literature are slightly different. The total widths inside the square brackets are estimated with the mixing angle $\theta_{1P}=-(55\pm5)°$.

$n^{2S+1}L_J$	State	Channel	Ours	XZ [55]	SSC [25]	LPW [27]	GI [26]	AMS [28]	$\Gamma_{\rm exp}$ [1]
1^3P_0	$B_0^*(5722)^+$	$B^+\pi^0+B^0\pi^+$	$97.5+195.5$					141.5	
		$B^{*+}\gamma$	477×10^{-3}				325×10^{-3}	575×10^{-3}	
		Total	293					142.08	
	$B_0^*(5722)^0$	$B^0\pi^0+B^+\pi^-$	$97.5+195.3$	272	225	230.43	154	141.5	
		$B^{*0}\gamma$	149×10^{-3}			116.9×10^{-3}	92.7×10^{-3}	175×10^{-3}	
		Total	292.8	272	225	230.43	154	141.7	
1^3P_2	$B_2^*(5747)^+$	$B^+\pi^0+B^0\pi^+$	$5.3+10.6$					9.77	
		$B^{*+}\pi^0+B^{*0}\pi^+$	$5.1+9.9$					9.79	
		$B^{*+}\gamma$	146×10^{-3}				444×10^{-3}	761×10^{-3}	
		Total	31				11.71	20.3	20 ± 5
	$B_2^*(5747)^0$	$B^0\pi^0+B^+\pi^-$	$5.5+10.8$	25	1.9	12.62	6.23	9.77	
		$B^{*0}\pi^0+B^{*+}\pi^-$	$5.2+10.2$	22	1.8	11.89	5.04	9.79	
		$B^{*0}\gamma$	51×10^{-3}			177.7×10^{-3}	126×10^{-3}	232×10^{-3}	
		Total	**32** (fitted)	47	3.7	24.51	11.40	19.8	24.2 ± 1.7
$1P$	$B_1(5680)^+$	$B^{*+}\pi^0+B^{*0}\pi^+$	$46.8+93.9$				163	125.53	
		$B^{*+}\gamma$	75×10^{-3}				300	448	
		$B^+\gamma$	111×10^{-3}				132×10^{-3}	415×10^{-3}	
		Total	140.9				163	126.4	128 ± 18
	$B_1(5680)^0$	$B^{*0}\pi^0+B^{*+}\pi^-$	$46.8+93.9$	219	200	199.4	163	125.53	
		$B^{*0}\gamma$	24×10^{-3}			53.1×10^{-3}	85.5×10^{-3}	137×10^{-3}	
		$B^0\gamma$	38×10^{-3}			130.2×10^{-3}	37.8×10^{-3}	127×10^{-3}	
		Total	140.8	219	200	199.4	163	125.8	128 ± 18
$1P'$	$B_1(5721)^+$	$B^{*+}\pi^0+B^{*0}\pi^+$	$13.8+27.4$				6.80	15.62	
		$B^{*+}\gamma$	206×10^{-3}				300×10^{-3}	339×10^{-3}	
		$B^+\gamma$	69×10^{-3}				132×10^{-3}	448×10^{-3}	
		Total	41.4 [24.5 ± 2.5]				7.27	16.4	31 ± 6
	$B_1(5721)^0$	$B^{*0}\pi^0+B^{*+}\pi^-$	$13.8+27.4$	30	10	40.63	6.80	15.62	
		$B^{*0}\gamma$	66×10^{-3}			108.5×10^{-3}	27.8×10^{-3}	103×10^{-3}	
		$B^0\gamma$	24×10^{-3}			60.4×10^{-3}	106×10^{-3}	137×10^{-3}	
		Total	41.3 [24.5 ± 2.5]	30	10	40.63	6.93	15.9	27.5 ± 3.4
1^3P_0	$B_{s0}^*(5788)^0$	$B^+K^-+B^0\bar{K}^0$	$86.7+76.7$	227	225		138	135.66	
		$B_s^{*0}\gamma$	102×10^{-3}			84.7×10^{-3}	76×10^{-3}	133×10^{-3}	
		Total	163.4	227	225		138	135.8	
1^3P_2	$B_{s2}^*(5840)^0$	$B^+K^-+B^0\bar{K}^0$	$0.69+0.61$	2		1.9	0.663	1.55	
		$B^{*+}K^-+B^{*0}\bar{K}^0$	$0.06+0.04$	0.12		0.14	0.00799	0.13	
		$B_s^{*0}\gamma$	51×10^{-3}			159×10^{-3}	106×10^{-3}	225×10^{-3}	
		Total	**1.31** (fitted)	2	0.26	1.66	0.777	1.9	1.49 ± 0.27
$1P$	$B_{s1}(5820)^0$	$B^{*+}K^-+B^{*0}\bar{K}^0$	⋯	149	120				
		$B_s^{*0}\gamma$	56×10^{-3}			39.5×10^{-3}	57.3×10^{-3}		
		$B_s^0\gamma$	37×10^{-3}			97.7×10^{-3}	47.8×10^{-3}		
		Total	0.093	149	120	160	0.1051		
$1P'$	$B_{s1}(5830)^0$	$B^{*+}K^-+B^{*0}\bar{K}^0$	$4.3+3.3$	0.4–1	∼0				
		$B_s^{*0}\gamma$	53×10^{-3}			98.8×10^{-3}	36.9×10^{-3}		
		$B_s^0\gamma$	27×10^{-3}			56.6×10^{-3}	70.6×10^{-3}		
		Total	7.6 [0.1–0.8]	0.4–1	∼0	20	0.1075		$0.5\pm0.3\pm0.3$

IV. DISCUSSION

A. 1P-wave states

Two $1P$-wave excited B meson states $B_1(5721)$ and $B_2^*(5747)^{+,0}$ together with their flavor partners $B_{s1}(5830)$ and $B_{s2}^*(5840)^0$ in the B_s-meson family have been well-established in experiments [1]. However, two resonances with $J^P=0^+$, $B(1^3P_0)$ and $B_s(1^3P_0)$, and two resonances with $J^P=1^+$, $B(P_1)$ and $B_s(P_1)$, predicted in the quark model are still missing.

1. 1^3P_2 states

There are no puzzles to assign the $B_2^*(5747)^{+,0}$ and $B_{s2}^*(5840)^0$ resonances to the 1^3P_2 states in the B and B_s families, respectively.

In the B meson sector, as the 1^3P_2 state both the mass and width of $B_2^*(5747)$ can be resonantly reproduced in the quark model. Our fitted mass $M \simeq 5727$ MeV and width $\Gamma \simeq 31$ MeV are compatible with the measurements $M_{\rm exp} = 5737$ MeV and width $\Gamma_{\rm exp} = (20 \pm 5)$ MeV for $B_2^*(5747)^+$. This state dominantly decays into $B\pi$ and $B^*\pi$ channels with comparable partial widths. The ideal partial width ratios between $B\pi$ and $B^*\pi$ channels for the $B_2^*(5747)^{+,0}$ are fitted to be

$$R_1 = \frac{\Gamma[B_2^*(5747)^0 \to B^{*+}\pi^-]}{\Gamma[B_2^*(5747)^0 \to B^+\pi^-]} \approx 0.94, \tag{19}$$

$$R_2 = \frac{\Gamma[B_2^*(5747)^+ \to B^{*0}\pi^+]}{\Gamma[B_2^*(5747)^+ \to B^0\pi^+]} \approx 0.93, \tag{20}$$

which are also consistent with the recent LHCb measurements $R_1^{\rm exp} = 0.71 \pm 0.14 \pm 0.30$ and $R_2^{\rm exp} = 1.0 \pm 0.5 \pm 0.8$ [8] and the predictions in Refs. [25,27,28,31–33,40,42].

We further study the radiative decay processes of $B_2^*(5747)^{+,0} \to B^{*+,0}\gamma$. Their partial decay widths are predicted to be

$$\Gamma[B_2^*(5747)^0 \to B^{*0}\gamma] = 51 \text{ keV}, \tag{21}$$

$$\Gamma[B_2^*(5747)^+ \to B^{*+}\gamma] = 146 \text{ keV}, \tag{22}$$

which are in good agreement with the predictions in Ref. [42], however, notably smaller than the predictions in Refs. [26–29,43]. The radiative decay branching fractions can reach up to $\mathcal{O}(10^{-3})$, thus radiative decays of $B_2^*(5747)^{+,0} \to B^{*+,0}\gamma$ might be observed in future experiments.

In the B_s meson sector, as the 1^3P_2 state both the mass and width of $B_{s2}^*(5840)$ can be well reproduced in the quark model as well. Our fitted mass $M \simeq 5821$ MeV and width $\Gamma \simeq 1.3$ MeV are compatible with the measured mass $M_{\rm exp} = 5840$ MeV and width $\Gamma_{\rm exp} = (1.49 \pm 0.27)$ MeV. There are two OZI allowed two-body strong decay channels BK and B^*K. The BK mode governs the decays of $B_{s2}^*(5840)$. The ideal partial width ratio between B^*K and BK is fitted to be

$$R = \frac{\Gamma[B_{s2}^*(5840) \to B^{*+}K^-]}{\Gamma[B_{s2}^*(5840) \to B^+K^-]} \approx 8.7\%, \tag{23}$$

which is in good agreement with the recent LHCb measured one $R^{\rm exp} = (9.3 \pm 2.5)\%$ [5] and the predictions in the literature [25,27–29,38].

Furthermore, it is found that $B_{s2}^*(5840)^0$ has a large decay rate into $B_s^*\gamma$, the partial width and branching fraction are predicted to be

$$\Gamma[B_{s2}^*(5840)^0 \to B_s^{*0}\gamma] \simeq 51 \text{ keV}, \tag{24}$$

$$\text{Br}[B_{s2}^*(5840)^0 \to B_s^{*0}\gamma] \simeq 3.4\%. \tag{25}$$

Our predicted radiative partial decay width is consistent with those predictions in Refs. [42,43]. In the literature, a larger partial width $\Gamma[B_{s2}^*(5840)^0 \to B_s^{*0}\gamma] \simeq 100$–$230$ keV is predicted [26–28]. The $B_s^{*0}\gamma$ decay channel of $B_{s2}^*(5840)^0$ may have good potentials to be observed in future experiments.

2. 1^3P_0 states

The 1^3P_0 states in the B and B_s families are still missing experimentally. In the B meson sector, we predict that the mass of the $B(1^3P_0)$ state is 5722 MeV, which is consistent with those predictions in Refs. [13,14,17,24,26,28]. The $B\pi$ channel is the only OZI-allowed two body decay channel. Taking the estimated mass $M = 5722$ MeV, we obtain a broad width $\Gamma \simeq 290$ MeV for the $B(1^3P_0)$ state, which is compatible with our previous result $\Gamma \simeq 270$ MeV predicted with the SHO wave functions in Ref. [55]. The $B(1^3P_0)$ state is also predicted to be a broad state with a width of ~150–250 MeV in the other models [25–27,29,31,41]. We also study the radiative decays of $B(1^3P_0)^{+,0}$, our results have been listed in Table V, the predicted partial width for $\Gamma[B(1^3P_0)^+ \to B^{*+}\gamma] \simeq 477$ keV is about a factor 3 larger than that for $\Gamma[B(1^3P_0)^0 \to B^{*0}\gamma] \simeq 149$ keV. Our predictions are comparable with those predicted in Refs. [26,28]. It should be mentioned that the radiative decays of $B(1^3P_0)^{+,0}$ are governed by the $E1$ transitions. For a heavy-light meson system, the $E1$ transition amplitude $\mathcal{A}$ is mainly contributed by the light quark, it is proportional to e_q/m_q, where e_q and m_q stands for the charge and mass of the light quark, respectively. The heavy quark contributions are strongly suppressed by the heavy quark mass m_Q (i.e., the factor $1/m_Q$). If neglecting the heavy quark contributions, one has $\Gamma[B(1^3P_0)^+ \to B^{*+}\gamma]$: $\Gamma[B(1^3P_0)^0 \to B^{*0}\gamma] = 4:1$, which is slightly larger than the ratio ~3 including heavy quark contributions.

In the B_s meson sector, the mass of $B_s(1^3P_0)$ is expected to be around 5788 MeV, which is compatible with those predictions in Refs. [12–14,17,24,26–28]. The BK channel is the only OZI-allowed two body strong decay channel. Taking the estimated mass $M = 5788$ MeV, we obtain a broad width $\Gamma \simeq 270$ MeV for the $B_s(1^3P_0)$ state. This prediction is compatible with our previous result $\Gamma \simeq 227$ MeV predicted with the SHO wave functions in Ref. [55]. The $B_s(1^3P_0)$ state is also predicted to be a broad state with a width of ~130–230 MeV in the other models [25,26,29]. We also study the radiative decay of $B_s(1^3P_0)$, the predicted partial width for $\Gamma[B_s(1^3P_0) \to B_s^{0*}\gamma] \simeq 100$ keV is close to the predictions in Refs. [26,28]. Finally, it should be mentioned that in some works [12,27,28], the predicted mass of $B_s(1^3P_0)$ is below the

BK mass threshold, which will lead to a very narrow width for the $B_s(1^3P_0)$ state.

3. $1^1P_1 - 1^3P_1$ mixing

The spin-orbit potential causes a strong configuration mixing between 1^3P_1 and 1^1P_1. It is generally believed that $B_1(5721)$ and $B_{s1}(5830)$ correspond to the mixed states $|1P_1'\rangle$ via the $1^1P_1 - 1^3P_1$ mixing in the B and B_s families, respectively. The other two mixed states $B_1(1P_1)$ and $B_{s1}(1P_1)$ in the B and B_s families are waiting to be established in future experiments.

Considering $B_1(5721)$ as the mixed state $|1P_1'\rangle$ defined in Eq. (9), our fitted mass $M = 5753$ MeV is reasonably comparable with the measured value $M_{\rm exp} = 5726$ MeV. With the mixing angle $\theta_{1P} = -35.2°$ determined from our quark model, the width of $B_1(5721)^0$ is predicted to be $\Gamma \simeq 41$ MeV, which is in good agreement with the predictions in Refs. [27,31], while slightly larger than the observed width $\Gamma_{\rm exp} \simeq 30$ MeV at LHC [8] and those predictions in Refs. [25,26,28,30]. The decay width is nearly saturated by the $B^*\pi$ channel. If we taking the mixing angle around the value obtained in the heavy-quark symmetry limit, i.e., $\theta_{1P} = -(55 \pm 5)°$ [55,93–97], the decay width is predicted to be in the range of $\Gamma = (24.5 \pm 2.5)$ MeV, which seems to be more comparable with the LHCb observations [8]. We also study the radiative decay processes of $B_1(5721) \to B^*\gamma, B\gamma$, their partial decay widths are predicted to be

$$\Gamma[B_1(5721)^0 \to B^{*0}\gamma/B^0\gamma] = 66/24 \text{ keV}, \quad (26)$$

$$\Gamma[B_1(5721)^+ \to B^{*+}\gamma/B^+\gamma] = 206/69 \text{ keV}. \quad (27)$$

Our predictions are comparable with those in Ref. [42], however, most of our predictions are notably smaller than the predictions in Refs. [26–28]. The radiative decay modes $B^*\gamma$ and $B\gamma$ of $B_1(5721)$ may be observed in future experiments since their branching fractions can reach up to the order of $O(10^{-3})$.

In the B-meson family, the mass for the other mixed state $B_1(1P_1)$ is about 40 MeV lower than that of $B_1(5721)$ according to our potential model calculations, which is consistent with the prediction in Ref. [24]. A slightly smaller mass splitting, $\sim(10 - 30)$ MeV, between $B_1(5721)$ and $B_1(1P_1)$ is given in Refs. [13,14,26–28]. Thus, the mass of $B_1(1P_1)$ might be in the range of (5700 ± 15) MeV. Considering the mass uncertainties, with the mixing angle $\theta_{1P} = -35.2°$ we plot the decay width of $B_1(1P_1)$ as a function of its mass in Fig. 3. It is found that $B_1(1P_1)$ is a broad state with a width of $\Gamma \simeq (155 \pm 10)$ MeV. The $B^*\pi$ channel is the only OZI-allowed two body strong decay channel. The $B_J(5732)$ listed in the RPP [1] is a good candidate for the $B_1(1P_1)$. With this assignment, both the measured mass $M_{\rm exp} = 5698$ MeV and width

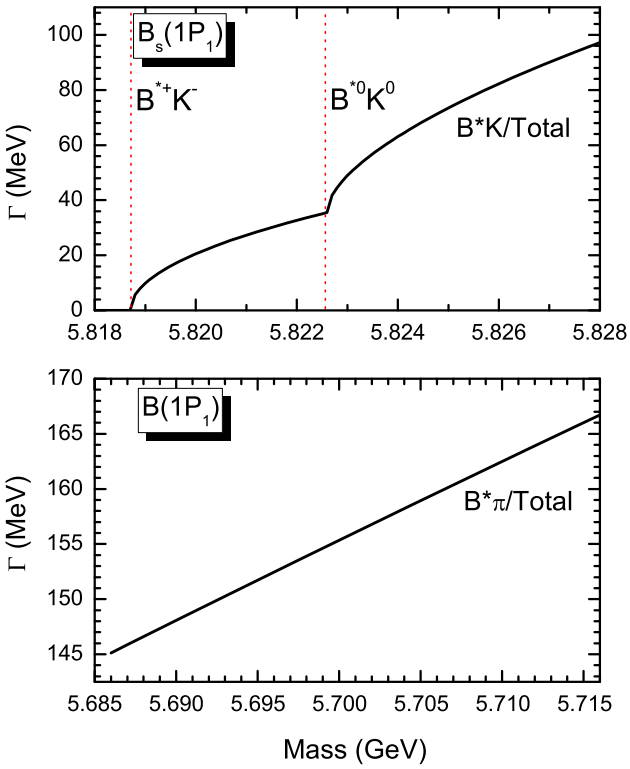

FIG. 3. Decay widths of the $1P$-wave mixed states $B_s(1P_1)$ and $B(1P_1)$ as a function of mass. The mixing angles for the $B_s(1P_1)$ and $B(1P_1)$ states are adopted the potential model predictions $\theta_{1P} = -39.6°$ and $-35.2°$, respectively.

$\Gamma_{\rm exp} = (128 \pm 18)$ MeV for the $B_J(5732)$ are in good agreement with the quark model predictions. However, in Ref. [23] the $B_J(5732)$ is assigned to the $B(1^3P_0)$ state according to the mass spectrum analysis.

As the mixed state $|1P_1'\rangle$, the mass of $B_{s1}(5830)$ is consistent with our fitted value $M = 5821$ MeV and other determinations in the literature (See Table IV). It dominantly decays into the B^*K channel. Taking the mixing angle $\theta_{1P} = -39.6°$ determined by our potential model, we find that the theoretical width, $\Gamma \simeq 7.6$ MeV, is too large to be comparable with the measured one $\Gamma_{\rm exp} \simeq (0.5 \pm 0.3 \pm 0.3)$ MeV. However, if we taking the mixing angle around the value obtained in the heavy-quark symmetry limit, i.e., $\theta_{1P} = -(55 \pm 5)°$, as that adopted in Ref. [55], the decay width is predicted to be in the range of $\Gamma = 0.08$–0.8 MeV, which is comparable with the data. It indicates that the mixing angle between 1^1P_1 and 1^3P_1 may be close to the value $\theta_{1P} = -55°$ obtained in the heavy-quark symmetry limit. The $B_{s1}(5830)$ has large decay rates into $B_s^*\gamma$ and $B_s\gamma$ channels. Their partial decay widths are predicted to be

$$\Gamma[B_{s1}(5830) \to B_s^*\gamma] = 53 \text{ keV}, \quad (28)$$

$$\Gamma[B_{s1}(5830) \to B_s\gamma] = 27 \text{ keV}. \quad (29)$$

The branching fractions of these radiative decays may reach up to $O(10^{-2})$. Our predictions are comparable with those predicted in Refs. [26,27,42]. The $B_s^*\gamma$ and $B_s\gamma$ decay channels of $B_{s1}(5830)$ may have good potentials to be observed in future experiments.

In the B_s meson sector, the mass of the other mixed state $B_{s1}(1P_1)$ is predicted to be about 2–40 MeV lower than that of $B_{s1}(5830)$ in various quark models [12–14,24,26–28]. Thus, the mass of $B_{s1}(1P_1)$ is estimated to be $\sim(5808 \pm 19)$ MeV, which is just around the $B^{*+}K^-$ and $B^{*0}K^0$ mass thresholds. From Fig. 3, it is seen that the strong decay properties of $B_{s1}(1P_1)$ are very sensitive to the mass threshold. There are three cases to be considered. (i) If the mass of $B_{s1}(1P_1)$ is below the $B^{*+}K^-$ mass threshold 5818 MeV, the radiative decay modes $B^*\gamma$ and $B\gamma$ may play crucial roles in the decays. The with partial decay widths are estimated to be

$$\Gamma[B_{s1}(1P_1) \to B_s^*\gamma] \simeq 60 \text{ keV}, \tag{30}$$

$$\Gamma[B_{s1}(1P_1) \to B_s\gamma] \simeq 40 \text{ keV}. \tag{31}$$

Then, the $B_{s1}(1P_1)$ should has a very narrow width of $\Gamma \sim \mathcal{O}(100)$ keV. (ii) If the mass of $B_{s1}(1P)$ lies between the $B^{*+}K^-$ mass threshold 5818 MeV and the $B^{*0}K^0$ mass threshold 5822 MeV, the $B_{s1}(1P_1)$ dominantly decays into $B^{*0}K^0$ mode, and has a narrow width of $\Gamma \simeq (20 \pm 15)$ MeV. (iii) If the mass of $B_{s1}(1P_1)$ is above the $B^{*0}K^0$ mass threshold 5822 MeV, the $B_{s1}(1P_1)$ dominantly decays into $B^{*0}K^0$ and $B^{*+}K^-$ channels, and has a relatively broad width of $\Gamma \simeq (70 \pm 30)$ MeV. It should be mentioned that the OPAL Collaboration observed some signals of a resonance denoted by $B_{sJ}(5850)$ with a mass of $M_{\rm exp} = (5853 \pm 15)$ MeV and a width of $\Gamma \simeq (47 \pm 22)$ MeV many year ago [98]. As a candidate of $B_{s1}(1P_1)$, both the measured mass and width of $B_{sJ}(5850)$ are consistent with the predictions. To confirm the $B_{sJ}(5850)$ resonance and established the $B_{s1}(1P_1)$ state, more observations of the $B^{*0}K^0$ and $B^{*+}K^-$ final states are suggested to be carried out in future experiments.

As a whole the high mass mixed state $|1P_1'\rangle$ via the $1^1P_1 - 1^3P_1$ mixing in the B and B_s families have been well established, they correspond to two narrow states $B_1(5721)$ and $B_{s1}(5830)$ observed in experiments. Some evidence for the low mass mixed states $|1P_1\rangle$ with broad widths predicted in theory may have been observed in experiments. The $B_J(5732)$ and $B_{sJ}(5850)$ resonances listed by the PDG [1] may good candidates for the missing $|1P_1\rangle$ in the B and B_s families, respectively.

B. 2S-wave states

1. 2^1S_0 states

The 2^1S_0 states in the B and B_s families are still not established. In the B meson sector, our predicted mass for the $B(2^1S_0)$ state is $M = 5876$ MeV, which is in agreement with the predictions in Refs. [14,24,26,28]. Taking the mass $M = 5876$ MeV, we calculate the strong and radiative decay properties of $B(2^1S_0)$, our results are listed in Table VI. The decays of $B(2^1S_0)$ are governed by the $B^*\pi$ mode with a fairly large branching fraction ~94%. The width of $B(2^1S_0)$ is predicted to be $\Gamma \simeq 63$ MeV, which is about a factor 1.5–4 larger than the predictions in Refs. [24,25,28,47], while about a factor 1.5–2 smaller than the predictions in Refs. [26,27,31,33].

In 2015, the LHCb Collaboration observed two new resonances $B_J(5840)^{0,+}$ [8]. Considering $B_J(5840)^{0,+}$ as unnatural parity states, the relatively accurate measurements of the mass and width for the neutral one are $M_{\rm exp} = (5863 \pm 9)$ MeV and $\Gamma_{\rm exp} = (127 \pm 51)$ MeV, respectively [8]. In this case, signals of $B_J(5840)^{0,+}$ should come from the $B^*\pi$ decay mode other than $B\pi$. In Refs. [18,26–28,39], the $B_J(5840)^{0,+}$ resonances were suggested to be the $B(2^1S_0)$ assignment. If $B_J(5840)^{0,+}$ have an unnatural parity indeed, they strongly favor the $B(2^1S_0)$ assignment. The measured mass and width together with the decay modes of $B_J(5840)$ are consistent with the our theoretical predictions. However, a natural parity for $B_J(5840)^{0,+}$ is also possible according to the LHCb analysis (see Case B listed in Table I). The $B_J(5840)^{0,+}$ may possibly decay into both the $B^*\pi$ and $B\pi$ channels. If the $B\pi$ decay mode is confirmed in future experiments, the $B_J(5840)$ resonance should be other assignments since the $B\pi$ mode is forbidden for the $B(2^1S_0)$ state.

In the B_s meson sector, our predicted mass for the $B_s(2^1S_0)$ state is $M = 5944$ MeV, which is comparable with the other quark model predictions [12–14,24,26–28]. Taking $M = 5944$ MeV, we calculate the strong and radiative decay properties of $B_s(2^1S_0)$, our results are listed in Table VI. The B^*K channel is the only OZI-allowed two body strong decay channel for $B_s(2^1S_0)$. Its decay width is predicted to be $\Gamma \simeq 55$ MeV, which is comparable with those predictions in Refs. [25,26,28,33,47]. The $B_s(2^1S_0)$ state should have large potentials to be seen in the $B^{*+}K^-$ channel since it has a fairly narrow width.

2. 2^3S_1 states

In the B meson sector, our predicted mass for $B(2^3S_1)$ is $M = 5899$ MeV, which is in good agreement with the predictions in Refs. [14,28]. Taking the mass $M = 5899$ MeV, we calculate the strong and radiative decay properties of $B(2^3S_1)$, our results are listed in Table VI. It is found that the $B(2^3S_1)$ state is a fairly narrow state with a width of $\Gamma \simeq 40$ MeV, which is consistent with the prediction in Refs. [25,47], however, a factor ~2–4 smaller than the predictions in Refs. [26,27,31,33]. This state dominantly decays into the $B^*\pi$ channel with a branching fraction ~54%. The partial width ratio between the two typical channels $B\pi$ and $B^*\pi$ is predicted to be

TABLE VI. Partial and total decay widths (MeV) for the $2S$-wave B and B_s mesons.

			Γth (MeV)			
$n^{2S+1}L_J$	State	Channel	$(b\bar{u}/b\bar{d})$	State	Channel	Γth (MeV)
2^1S_0	$B_0(5876)$	$B^*\pi$	59	$B_{s0}(5944)$	B^*K	55
		$B^*\eta$	0.05		$B_s^*\eta$	⋯
		$B(1^3P_0)\pi$	4.8		$B_s^*\gamma$	0.1×10^{-3}
		$B^*\gamma$	$0.006/0.85\times10^{-3}$		$B_s(1P)\gamma$	0.009
		$B(1P)\gamma$	0.1/0.034		$B_{s1}(5830)\gamma$	4.9×10^{-3}
		$B_1(5721)\gamma$	$0.026/8.8\times10^{-3}$		Total	55
		Total	63			
2^3S_1	$B_1(5899)$	$B\pi$	5.1	$B_{s1}(5966)$	BK	15
		$B\eta$	0.8		$B_s\eta$	0.1
		B_sK	0.02		B^*K	32
		$B^*\pi$	22		$B_s^*\eta$	0.01
		$B^*\eta$	0.6		$B_s\gamma$	3.6×10^{-3}
		$B_2(5747)\pi$	<0.01		$B_s(2^1S_0)\gamma$	1.0×10^{-6}
		$B(1P)\pi$	11		$B_{s2}(5840)\gamma$	9×10^{-3}
		$B_1(5721)\pi$	1		$B_s(1P)\gamma$	2.2×10^{-3}
		$B\gamma$	0.029/0.008		$B_{s1}(5830)\gamma$	2.7×10^{-3}
		$B(2^1S_0)\gamma$	$6\times10^{-5}/2\times10^{-5}$		$B(1^3P_0)\gamma$	1.4×10^{-3}
		$B_2(5747)\gamma$	0.06/0.019		Total	47
		$B(1P)\gamma$	$0.015/5.2\times10^{-3}$			
		$B_1(5721)\gamma$	$0.018/6.2\times10^{-3}$			
		$B(1^3P_0)\gamma$	$0.004/1.6\times10^{-3}$			
		Total	41			

$$\frac{\Gamma[B\pi]}{\Gamma[B^*\pi]}\simeq 0.23, \tag{32}$$

which can be used to identify the $B(2^3S_1)$ from its possible candidates observed in future experiments.

It should be mentioned that the $B_J(5840)$ resonance may be a candidate of the $B(2^3S_1)$ state as suggested in Refs. [29,31]. As this assignment, both the mass and typical decay modes $B^*\pi$ and $B\pi$ predicted in theory are consistent with the LHCb observations [8]. Our predicted width $\Gamma\simeq 41$ MeV is close to the lower limit of the measured width $\Gamma_{\rm exp}=(107\pm54)$ MeV assuming a natural parity for $B_J(5840)^0$ [8]. Furthermore, the $B_J(5970)$ resonance was also suggested to be the $B(2^3S_1)$ state in the literature [18,25–27,33,35]. The $B_J(5970)^{0,+}$ resonances were first observed by the CDF Collaboration in the $B\pi$ final states in 2013 [7], and confirmed by the LHCb Collaboration two years later [8]. The central value of the measured width is $\Gamma_{\rm exp}\simeq$ 60–70 MeV with large uncertainties (see Table I). In the LHCb observations, the $B^*\pi$ decay mode has been seen, while the $B\pi$ mode may be possibly seen [1]. If assigning $B_J(5970)$ resonance to $B(2^3S_1)$, our predicted mass, $M\simeq 5899$ MeV, is about 70 MeV larger than the observation, while the predicted width, $\Gamma\simeq 54$ MeV, is consistent with the data. As a conclusion, we cannot exclude the possibilities of the $B_J(5840)$ and $B_J(5970)$ resonances as candidates of the $B(2^3S_1)$ state based on the present experimental information.

In the B_s meson sector, our predicted mass for the $B_s(2^3S_1)$ state is $M=5966$ MeV, which is in good agreement with the predictions in Refs. [12,14,28]. Taking $M=5966$ MeV, we calculate the strong and radiative decay properties of $B_s(2^3S_1)$, our results are listed in Table VI. It is found that the $B_s(2^3S_1)$ state is also a narrow state with a width of $\Gamma\simeq 50$ MeV, which is consistent with the predictions in Refs. [25,47], however, a factor ∼2–4 smaller than the predictions in Refs. [26,27,33]. This state mainly decays into the B^*K and BK channel with large branching fractions ∼68% and ∼32%, respectively. The partial width ratio between the two main channels BK and B^*K is predicted to be

$$\frac{\Gamma[BK]}{\Gamma[B^*K]}\simeq 0.47, \tag{33}$$

which may be an important criterion for establishing the $B_s(2^3S_1)$.

There may exist a strong configuration mixing between the 2^3S_1 and 1^3D_1 states, which is to be discussed in the last part of this section.

C. 1D-wave states

Some evidence of the $1D$-wave B and B_s states may have been observed in experiments. The $B(5970)^{0,+}$ together

TABLE VII. Partial and total decay widths (MeV) for the $1D$-wave B and B_s mesons.

	Observed State		Γth (MeV)	Observed State		
$n^{2S+1}L_J$	B meson	Channel	$(b\bar{u}/b\bar{d})$	B_s meson	Channel	Γth (MeV)
1^3D_3	$B_3^*(5979)$	$B\pi$	17	$B_{s3}^*(6067)$	BK	7.0
		$B\eta$	0.2		$B_s\eta$	0.1
		B_sK	0.1		B^*K	5.8
		$B^*\pi$	17		$B_s^*\eta$	0.03
		$B^*\eta$	0.1		$B_{s2}(5840)\gamma$	0.038
		B_s^*K	0.01		$B_{s1}(5830)\gamma$	2.0×10^{-4}
		$B_2(5747)\pi$	0.9		$B_s(1P_1)\gamma$	2.0×10^{-4}
		$B_1(5721)\pi$	0.01		$B_s(1^3P_0)\gamma$	1.0×10^{-4}
		$B(1P_1)\pi$	3.6		Total	13
		$B_2(5747)\gamma$	0.125/0.043			
		$B_1(5721)\gamma$	$1.9\times10^{-3}/0.5\times10^{-3}$			
		$B(1P_1)\gamma$	$1.9\times10^{-3}/0.5\times10^{-3}$			
		$B(1^3P_0)\gamma$	$0.7\times10^{-3}/0.2\times10^{-3}$			
		Total	39			
1^3D_1	$B_1^*(6056)$	$B\pi$	92	$B_{s1}^*(6101)$	BK	87
		$B\eta$	14		$B_s\eta$	7.3
		B_sK	21		B^*K	37
		$B^*\pi$	41		$B_s^*\eta$	2.6
		$B^*\eta$	5.3		$B_{s2}(5840)\gamma$	3.9×10^{-3}
		B_s^*K	7.3		$B_s(1P_1)\gamma$	0.017
		$B_2(5747)\pi$	2.1		$B_{s1}(5830)\gamma$	0.023
		$B_1(5721)\pi$	148		$B_s(1^3P_0)\gamma$	0.044
		$B(1P)\pi$	20		Total	133
		$B_2(5747)\gamma$	0.035/0.01			
		$B(1P)\gamma$	0.122/0.039			
		$B_1(5721)\gamma$	0.178/0.056			
		$B(1^3P_0)\gamma$	0.201/0.066			
		Total	350			
$1D_2'$	$B_2(6067)$	$B^*\pi$	66	$B_{s2}(6113)$	B^*K	22
		$B^*\eta$	1.7		$B_S^*\eta$	0.5
		B_s^*K	1.4		$B_{s2}(5840)\gamma$	0.016
		$B(1^3P_0)\pi$	3.5		$B_s(1P)\gamma$	1.3×10^{-3}
		$B_2(5747)\pi$	6.2		$B_{s1}(5830)\gamma$	0.064
		$B_1(5721)\pi$	10		$B_s(1^3P_0)\gamma$	3.0×10^{-4}
		$B(1P)\pi$	0.4		Total	23
		$B_2(5747)\gamma$	0.106/0.033			
		$B(1P)\gamma$	$0.022/6.5\times10^{-3}$			
		$B_1(5721)\gamma$	0.302/0.104			
		$B(1^3P_0)\gamma$	$3.3\times10^{-3}/1.0\times10^{-3}$			
		Total	90			
$1D_2$	$B_2(5973)$	$B^*\pi$	92	$B_{s2}(6061)$	B^*K	85
		$B^*\eta$	6.7		$B_S^*\eta$	4.2
		B_s^*K	5.2		$B_{s2}(5840)\gamma$	6.0×10^{-3}
		$B(1^3P_0)\pi$	0.002		$B_s(1P)\gamma$	0.045
		$B_2(5747)\pi$	64		$B_{s1}(5830)\gamma$	0.5×10^{-3}
		$B(1P)\pi$	0.4		$B_s(1^3P_0)\gamma$	0.1×10^{-3}
		$B_1(5721)\pi$	0.04		Total	90
		$B_2(5747)\gamma$	0.026/0.008			
		$B(1P)\gamma$	0.223/0.076			
		$B_1(5721)\gamma$	$1.2\times10^{-3}/0.3\times10^{-3}$			
		$B(1^3P_0)\gamma$	$0.5\times10^{-3}/0.2\times10^{-3}$			
		Total	169			

with the new resonances $B_{sJ}(6064)$ and $B_{sJ}(6114)$ observed at LHCb may be good candidates of the $1D$-wave states according to the mass spectrum predictions in various quark models.

1. 1^3D_3 states

In Ref. [47], by analyzing the decay properties within the chiral quark model our group found that the $B_J(5970)$ is most likely to be the 1^3D_3 assignment in the B-meson family. The $B_J(5970)$ as a candidate of $B(1^3D_3)$ is also suggested in Refs. [27,31]. In present work, we restudy the $B_J(5970)$ by combining the decay properties with the mass spectrum. It is found that as the $B(1^3D_3)$ assignment the mass of $B(5970)$ can be well explained with the potential model. Our predicted mass $M = 5979$ MeV is in good agreement with the observed value $M_{\rm exp} = (5971 \pm 5)$ MeV for the neutral state $B(5970)^0$ [1]. By using the wave function of $B(1^3D_3)$ calculated from the potential model, we further study the decay properties, our results are listed in Table VII. It is found that the predicted decay width, $\Gamma \simeq 39$ MeV, is also consistent the measured width $\Gamma_{\rm exp} \simeq (56 \pm 16)$ MeV of $B(5970)^0$ by assuming $P = (-1)^J$ and using three relativistic Breit-Wigner functions in the fit for mass difference at LHCb [8]. The partial width ratio between $B\pi$ and $B^*\pi$ is predicted to be

$$\frac{\Gamma[B\pi]}{\Gamma[B^*\pi]} \simeq 1.0, \tag{34}$$

which is waiting to be tested in future experiments. If the $B_J(5970)^{0,+}$ resonances correspond to the $B(1^3D_3)$ assignment indeed, the charged state $B_J(5970)^+$ should have a large radiative decay rate into $B_2^*(5747)^+\gamma$, the partial width and branching fraction are predicted to be

$$\Gamma[B_J(5970)^+ \to B_2^*(5747)^+\gamma] \simeq 125 \text{ keV}, \tag{35}$$

$$\mathrm{Br}[B_J(5970)^+ \to B_2^*(5747)^+\gamma] \simeq 3 \times 10^{-3}. \tag{36}$$

The radiative decay mode $B_2^*(5747)^+\gamma$ may be observed in future experiments.

In Ref. [47], considering the $B_J(5970)$ as the $B(1^3D_3)$ assignment, our group further predicted that the mass and width of the $B_s(1^3D_3)$ state, as a flavor partner of $B_J(5970)$, might be $M \simeq 6.07$ GeV and $\Gamma \simeq 30$ MeV, respectively. The predicted mass of $B_s(1^3D_3)$ is consistent with the those predicted in Refs. [12,27,28], while a relatively narrow width is also predicted by other works [25–28,33,35]. It is interestingly found that the new bottom-strange structure $B_{sJ}(6064)$ with a mass of $M_{\rm exp} = (6063.5 \pm 2.0)$ MeV and a very narrow width of $\Gamma_{\rm exp} = (26 \pm 8)$ MeV observed at LHCb [9] is consistent with the predictions. In present work, from the aspects of both mass spectrum and decay properties we further discuss the possibility of the $B_{sJ}(6064)$ structure as the $B_s(1^3D_3)$ assignment in the B_s-meson family. With this assignment, it is found that the measured mass for the $B_{sJ}(6064)$ structure is consistent with the theoretical mass $M = 6067$ MeV. Furthermore, the narrow width of $B_{sJ}(6064)$ can also be explained within our chiral quark model. From our predicted decay properties listed in Table VII, it is found that the theoretical width $\Gamma \simeq 13$ MeV is close to lower limit of the measured value $\Gamma_{\rm exp} = (26 \pm 8)$ MeV from LHCb [9]. The partial width ratio between BK and B^*K is predicted to be

$$\frac{\Gamma[BK]}{\Gamma[B^*K]} \simeq 1.2. \tag{37}$$

Our predicted mass and decay properties of $B_s(1^3D_3)$ are compatible with those predicted in Refs. [27,28,47]. It should be pointed out that the large branching fraction for $\mathrm{Br}[B_{sJ}(6064) \to B^*K] \simeq 45\%$ seems to be not consistent with the observations naturally. Since $B_{sJ}(6064)$ causes a clear bump structure around 6064 MeV in the B^+K^- mass spectrum through the B^+K^- decay, it should also cause another narrow bump structure around 6019 MeV through the $B^{*+}K^-$ decay with a missing photon from $B^{*+} \to B^+\gamma$, however, this structure was not observed at LHCb. Thus, it indicates that the $B_s(1^3D_3)$ may not be the main contributor to the $B_{sJ}(6064)$ structure observed in the B^+K^- mass spectrum.

As a whole, the $B_J(5970)$ may be assigned as the 1^3D_3 assignment, which can be tested by the partial width ratio between $B\pi$ and $B^*\pi$. It may be a flavor partner of the $D_3^*(2750)$ and $D_{s3}(2860)$ resonances listed in RPP [1]. Their masses might be systematically overestimated by a value of ~100 MeV in some quark models [11,14,26,99]. There still exists a puzzle to identify the $B_{sJ}(6064)$ structure as the $B_s(1^3D_3)$ state, although both the predicted mass and width seem to be consistent with the observations. To establish the narrow $B_s(1^3D_3)$ state finally, the observations of both the B^+K^- and $B^{*+}K^-$ decays and their partial width ratio are crucial in future experiments.

2. 1^3D_1 states

In the B meson sector, the mass for the $B(1^3D_1)$ state is predicted to be $M = 6056$ MeV in our potential model calculations, which is comparable with the predictions in Refs. [13,24,27,28]. Our predicted mass for $B(1^3D_1)$ is about 80 MeV larger than that for $B(1^3D_3)$. Taking the mass $M = 6056$ MeV, we calculate the strong and radiative decay properties of $B(1^3D_1)$, our results are listed in Table VII. It is found that the $B(1^3D_1)$ state is a broad state with a width of $\Gamma \simeq 350$ MeV, which is consistent with the predictions in Refs. [25,27]. This state mainly decays into the $B\pi$, $B^*\pi$, and $B_1(5721)\pi$ channels with branching fractions ~26%, 12%, and 42%, respectively. The partial

width ratio between the two typical channels $B\pi$ and $B^*\pi$ is predicted to be

$$\frac{\Gamma[B\pi]}{\Gamma[B^*\pi]} \simeq 2.2, \tag{38}$$

which may be helpful to identify the $B(1^3D_1)$ state from future observations. In Refs. [28,29], $B_J(5970)$ was suggested to be a candidate for $B(1^3D_1)$. With this assignment we find that the theoretical width $\Gamma \simeq 230$ MeV is too broad to be comparable with the measured value measured value $\Gamma_{\rm exp} \simeq 60$–$70$ MeV (see Table I). Thus, $B_J(5970)$ may not be a good candidate of the 1^3D_1 state.

In the B_s meson sector, the mass for the $B_s(1^3D_1)$ state is predicted to be $M = 6101$ MeV in our potential model calculations, which is comparable with the predictions in Refs. [13,24,27]. Our predicted mass for $B_s(1^3D_1)$ is about 30 MeV larger than that of $B_s(1^3D_3)$. There are large uncertainties in the predictions of the mass splitting between $B_s(1^3D_1)$ and $B_s(1^3D_3)$. In some works [12,13,28], the $B_s(1^3D_1)$ mass is even predicted to be smaller than that of $B_s(1^3D_3)$. Taking the mass $M = 6101$ MeV, we calculate the strong and radiative decay properties of $B_s(1^3D_1)$, our results are listed in Table VII. It is found that the $B_s(1^3D_1)$ state has a width of $\Gamma \simeq 130$ MeV, and mainly decays into the BK and B^*K channels with branching fractions ~65% and 27%, respectively. The partial width ratio between the two typical channels BK and B^*K is predicted to be

$$\frac{\Gamma[BK]}{\Gamma[B^*K]} \simeq 2.4, \tag{39}$$

which is comparable with the predictions in Refs. [25,27]. From the point of view of mass, the observed resonance $B_{sJ}(6114)$ by the LHCb Collaboration [9] is a good candidate for the $B_s(1^3D_1)$ state. While, the theoretical width $\Gamma \simeq 130$ MeV is also close the upper limit of the measured width $\Gamma_{\rm exp} = (66 \pm 39)$ MeV. There may exist a configuration mixing between the 2^3S_1 and 1^3D_1 states, which will be discussed in the last part of this section.

3. $1^1D_2 - 1^3D_2$ mixing

There is a strong configuration mixing between the 1^3D_2 and 1^1D_2 states for the heavy-light mesons predicted in the potential models. For the B meson sector, with the mixing scheme defined in Eq. (9) the mixing angle is predicted to be $\theta_{1D} = -39.5°$, which is close to the value $-50.8°$ extracted in the heavy quark symmetry limit [25,95,96]. Our predicted masses for the $B(1D_2)$ and $B(1D_2')$ states are about 5973 and 6067 MeV, respectively, which are close to the predictions in Refs. [13,24]. A fairly large mass splitting between $B(1D_2)$ and $B(1D_2')$, $\Delta M = 94$ MeV, is obtained in present work. It is comparable with the predictions of $\Delta M = 110$–130 MeV in Refs. [26,27]. With the masses and wave functions obtained from our potential model calculations, the decay properties for these two mixed states $B(1D_2)$ and $B(1D_2')$ are estimated, the results are listed in Table VII. It is found that the low mass state $B(1D_2)$ has a broad width of $\Gamma \simeq 170$ MeV, and dominantly decays into $B^*\pi$ and $B_2^*(5747)\pi$ channels with branching fractions about 54% and 38%, respectively. While the high mass state $B(1D_2')$ has a relatively narrow width of $\Gamma \simeq 90$ MeV, and dominantly decays into $B^*\pi$, $B_1(5721)\pi$ and $B_2^*(5747)\pi$ channels with branching fractions about 73%, 11% and 7%, respectively. Our predicted decay properties are roughly comparable with those predictions in Refs. [25,26,47].

For the B_s meson sector, we predict the mixing angle $\theta_{1D} = -39.9°$. Our predicted masses for the $B_s(1D_2)$ and $B_s(1D_2')$ states are about 6061 and 6113 MeV, respectively, which are close to the predictions in Refs. [12,24,27]. An intermediate mass splitting between $B_s(1D_2)$ and $B_s(1D_2')$, $\Delta M = 52$ MeV, is obtained in present work, which is comparable with the predictions of $\Delta M = 45$–70 MeV in Refs. [24,27]. With the masses and wave functions obtained from our potential model calculations, the decay properties for these two mixed states $B_s(1D_2)$ and $B_s(1D_2')$ are estimated, the results are listed in Table VII. It is found that the low mass state $B_s(1D_2)(6061)$ has an intermediate width of

$$\Gamma \simeq 90 \text{ MeV}, \tag{40}$$

and dominantly decays into B^*K channel with a branching fraction about 94%. Our predicted width is about a factor 1.5–2 smaller than those predictions in Refs. [25–28]. The $B_s(1D_2)$ state may be observed around 6016 MeV in the B^+K^- mass spectrum through the $B^{*+}K^-$ decay with a missing photon from $B^{*+} \to B^+\gamma$.

While the high mass state $B_s(1D_2')(6113)$ has a very narrow width of

$$\Gamma \simeq 23 \text{ MeV}, \tag{41}$$

and dominantly decays into B^*K channel with a branching fraction about 95%. The decay properties predicted in present work are in good agreement with those predictions in Refs. [25,26,28,47]. The narrow mixed state $B_s(1D_2')$ with a mass of $M = 6113$ MeV may be the main contributor to the $B_{sJ}(6064)$ structure observed in the B^+K^- mass spectrum at LHCb [9]. In this case, the signal in the B^+K^- mass spectrum may mainly come from the $B^{*+}K^-$ decay with a missing photon from $B^{*+} \to B^+\gamma$. Including the energy of the missing photon, the mass and width are determined to be $M_{\rm exp} = (6109 \pm 1.8)$ MeV and $\Gamma_{\rm exp} = (22 \pm 9)$ MeV for the resonance $B_{sJ}(6109)$ [9]. It is interestingly found that the $B_{sJ}(6109)$ resonance favors the assignment of the $1D$-wave mixed state $B_s(1D_2')$. The predicted mass, width, decay mode are in good agreement

with the observations. Finally, it should be mentioned that the $B_s(1^3D_3)$ state may have a few contributions to the $B_{sJ}(6064)$ structure through the B^+K^- decay as well, since this state with a mass of $M \simeq 6067$ MeV lies just around the peak position.

D. $2^3S_1 - 1^3D_1$ mixing

It should be mentioned that there may exist a configuration mixing between the 2^3S_1 and 1^3D_1 states. To explain the strong decay properties of the $D_J^*(2600)$ and/or $D_{s1}(2700)$, configuration mixing between 2^3S_1 and 1^3D_1 is suggested in the literature [100–104]. In Refs. [53,54], our group also carefully studied the strong decay properties of the $D_J^*(2600)$ and $D_{s1}(2700)$. According the analysis, both $D_J^*(2600)$ and $D_{s1}(2700)$ could be explained as the mixed state $|SD\rangle_L$ via the $2^3S_1 - 1^3D_1$ mixing with the following mixing scheme:

$$\begin{pmatrix} |SD\rangle_L \\ |SD\rangle_H \end{pmatrix} = \begin{pmatrix} \cos\theta & \sin\theta \\ -\sin\theta & \cos\theta \end{pmatrix} \begin{pmatrix} 2^3S_1 \\ 1^3D_1 \end{pmatrix}, \quad (42)$$

where the mixed angle is estimated to be $\theta \simeq -(45 \pm 16)°$. The $D_{s1}(2860)$ resonance observed in the BK final state at LHCb [105,106] seems to be the high mass mixed state $|SD\rangle_H$ as the partner of the low mass state $D_{s1}(2700)$ [47], from which one can estimate a mass splitting $\Delta M \simeq 150$ MeV between the high and low mass mixed states. Similarly, the $2^3S_1 - 1^3D_1$ mixing might also exist in the B and B_s meson families.

The strong decay properties for the mixed states $|SD\rangle_L$ and $|SD\rangle_H$ in the B and B_s meson families were studied in another work of our group [47]. It is interestingly found that the newly observed resonances $B_J(5840)$ and $B_{sJ}(6114)$ at LHCb [8,9] are most likely to be the mixed states $B(|SD\rangle_L)$ and $B_s(|SD\rangle_H)$, respectively, by comparing the measured masses and widths with the theoretical predictions (see Figs. 1 and 2 in Ref. [47]).

Considering the $B_J(5840)$ resonance as the low mass mixed state $B(|SD\rangle_L)$, we revise the strong decay properties by using the wave functions obtained from our quark potential model calculations. Our results are shown in Fig. 4. With the mixing angle $\theta \simeq -(45 \pm 16)°$ determined in Refs. [53,54] and the mass $M_{\rm exp} \simeq 5890$ MeV measured at LHCb [8], the $B(|SD\rangle_L)$ state has a width of $\Gamma \simeq (76 \pm 20)$ MeV, and dominantly decays into $B^*\pi$ channel. There may be a sizeable decay rate into the $B\pi$ channel. The partial width ratio between $B\pi$ and $B^*\pi$ is predicted to be

$$\frac{\Gamma[B\pi]}{\Gamma[B^*\pi]} \simeq 0.1 - 0.7, \quad (43)$$

which is sensitive to the mixing angle. The predicted width is consistent with the measured width $\Gamma_{\rm exp} = (107 \pm 54)$ MeV by assuming $P = (-1)^J$. Moreover, the predicted decay modes are also consistent with the observations of $B_J(5840)$. To better understand the nature of $B_J(5840)$, more accurate measurements of the width together with the partial width ratio are expected to be carried out in future experiments.

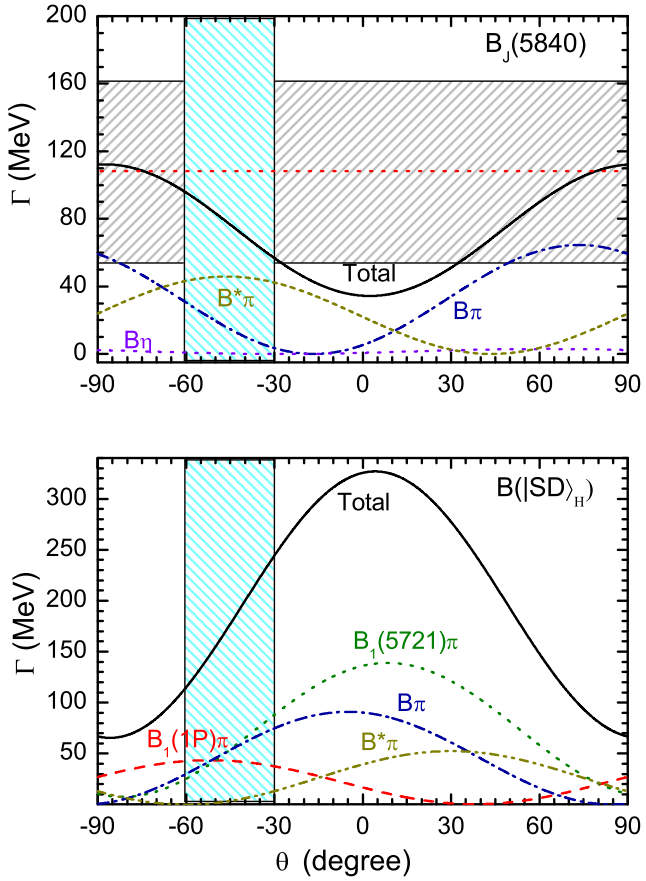

FIG. 4. The partial decay widths and total decay widths for the mixed states via $2^3S_1 - 1^3D_1$ mixing in the B-meson family as functions of the mixing angle θ. In the horizontal direction, the shaded region represents the possible range of the measured width from LHCb. In the vertical direction, shaded region represents the possible range of the mixing angle $\theta \simeq -(45 \pm 16)°$ suggested in Refs. [53,54]. The masses for $B_J(5840)$ and $B(|SD\rangle_H)$ are taken to be 5890 and 6040 MeV, respectively.

If $B_J(5840)$ corresponds to the low mass state $B(|SD\rangle_L)$ indeed, the mass of $B(|SD\rangle_H)$ may be about 150 MeV larger than that of $B_J(5840)$. Taking a mass of $M \simeq 6040$ MeV for $B(|SD\rangle_H)$, we show its decay properties in Fig. 4 as well. Within the mixing angle range $\theta \simeq -(45 \pm 16)°$ suggested in [53,54], the $B(|SD\rangle_H)$ has a width of $\Gamma \simeq (197 \pm 47)$ MeV, and mainly decay into $B\pi$ and $B_1(5721)\pi$ channels. The partial width ratio between $B\pi$ and $B_1(5721)\pi$ is predicted to be

$$\frac{\Gamma[B\pi]}{\Gamma[B_1(5721)\pi]} \sim 1, \quad (44)$$

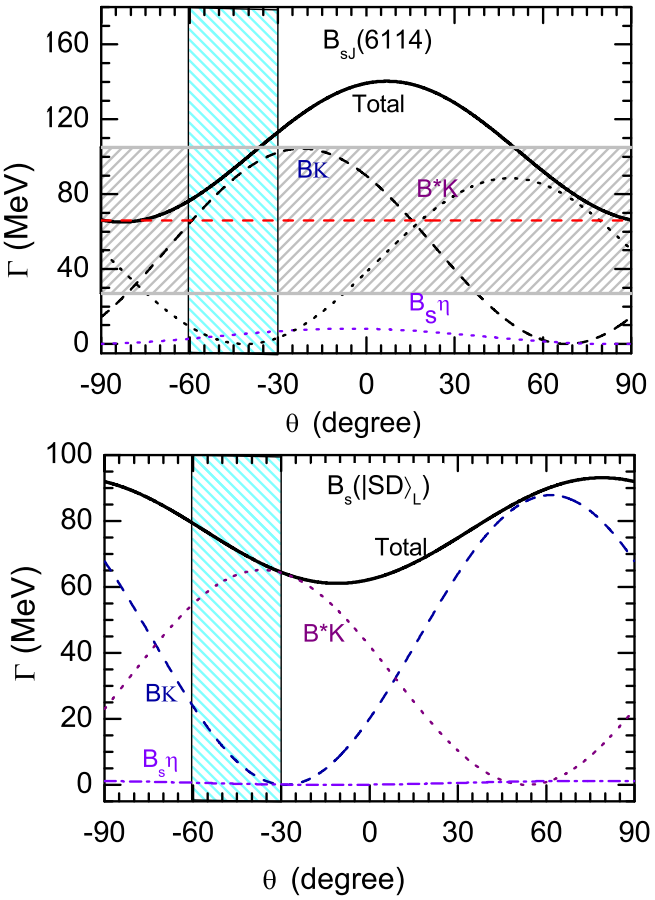

FIG. 5. The partial decay widths and total decay widths for the mixed states via $2^3S_1 - 1^3D_1$ mixing in the B_s-meson family as functions of the mixing angle θ. In the horizontal direction, the shaded region represents the possible range of the measured width from LHCb. In the vertical direction, shaded region represents the possible range of the mixing angle $\theta \simeq -(45 \pm 16)°$ suggested in Refs. [53,54]. The masses for $B_{sJ}(6114)$ and $B_s(|SD\rangle_L)$ are taken to be 6114 and 5964 MeV, respectively.

which is insensitive to the mixing angle. Future observations in the $B\pi$ channel with a larger data sample at LHCb may have a potential to discover this high mass mixed state $B_1(|SD\rangle_H)$.

In the B_s meson sector, considering the $B_{sJ}(6114)$ resonance observed in the B^+K^- mass spectrum [9] as the high mass mixed state $B_s(|SD\rangle_H)$, we revise the strong decay properties by using the wave functions obtained from our quark potential model calculations. Our results are shown in Fig. 5. It is found that with the mixing angle $\theta \simeq -(45 \pm 16)°$ determined in Refs. [53,54], the $B_s(|SD\rangle_H)$ state has a width of $\Gamma \simeq (95 \pm 15)$ MeV, and dominantly decays into BK channel with a branching fraction ~90%. Both the decay mode B^+K^- and width $\Gamma_{\rm exp} = (66 \pm 39)$ MeV observed for $B_{sJ}(6114)$ at LHCb [9] can be well understood in our quark model calculations. Thus, the $B_{sJ}(6114)$ may favor the mixed state $B_s(|SD\rangle_H)$.

The mass for the low mass state $B_{s1}(|SD\rangle_L)$ may be about 150 MeV smaller than that of $B_{sJ}(6114)$. Taking a mass of $M \simeq 5960$ MeV for the low mass state $B_{s1}(|SD\rangle_L)$, we show its decay properties in Fig. 5 as well. In the mixing angle range $\theta \simeq -(45 \pm 16)°$, the $B_{s1}(|SD\rangle_L)$ has a width of $\Gamma \simeq (70 \pm 10)$ MeV, and mainly decay into B^*K channel. The partial width ratio between BK and B^*K,

$$\frac{\Gamma[BK]}{\Gamma[B^*K]} < 0.5, \tag{45}$$

is sensitive to the mixing angle. The $B_{s1}(|SD\rangle_L)$ is most likely to be observed in the B^+K^- final state with a larger data sample at LHCb.

As a whole the $B_J(5840)$ and $B_{sJ}(6114)$ may favor the mixed states $B(|SD\rangle_L)$ and $B_s(|SD\rangle_H)$ via $2^3S_1 - 1^3D_1$ mixing, respectively. Their partners $B(|SD\rangle_H)$ and $B_s(|SD\rangle_L)$ are expected to be observed in their dominant decay channels with a larger data sample at LHCb.

V. SUMMARY

The experimental progress provides us good opportunities to establish an abundant B and B_s-meson spectrum up to the second orbital excitations. In this work, combining the newest experimental progress, we carry out a systematical study of the mass spectrum, strong decays and radiative decays of the $1P$-, $1D$-, and $2S$-wave excited B and B_s states in the constitute quark model. The mass and strong decay properties for the well established $1P$-wave resonances $B_1(5721)^{+,0}$, $B_2^*(5747)^{+,0}$, $B_{s1}(5830)$ and $B_{s2}^*(5840)$ can be consistently explained. The possible assignments for the high mass resonances/structures $B_J(5840)^{0,+}$, $B(5970)^{0,+}$, $B_{sJ}(6064)$ and $B_{sJ}(6114)$ are discussed. We hope that our study can provide some useful information toward establishing an abundant B and B_s-meson spectrum. Our main results are summarized as follows.

For the P-wave states, several points should be emphasized. (i) Some radiative decay processes, such as $B_{s1}(5830) \to B_s^{(*)}\gamma$ and $B_{s2}^*(5840) \to B_s^*\gamma$, have good potentials to be found in future experiments due to their fairly branching fractions of $\mathcal{O}(10^{-2})$. (ii) The $B_J(5732)$ and $B_{sJ}(5850)$ resonances listed by the PDG [1] may good candidates for the missing $|1P_1\rangle$ state in the B and B_s families, respectively. (iii) Both $B(1^3P_0)$ and $B_s(1^3P_0)$ may hardly be observed in experiments due to their very broad width of $\Gamma \sim 300$ MeV.

The $B_J(5840)$ resonance and the new $B_{sJ}(6114)$ structure observed in the B^+K^- mass spectrum may be explained with the mixed states $B(|SD\rangle_L)$ and $B_s(|SD\rangle_H)$ via $2^3S_1 - 1^3D_1$ mixing, respectively. To confirm the nature of the $B_J(5840)$ and $B_{sJ}(6114)$, the typical ratios $\Gamma(B\pi)/\Gamma(B^*\pi)$ and $\Gamma(B^*K)/\Gamma(BK)$ are suggested to be measured in future

experiments. The other two missing states, $B(|SD\rangle_H)$ with a mass of $M \simeq 6010$ MeV and $B_s(|SD\rangle_L)$ with a mass of $M \simeq 5960$ MeV, may be observed in the $B\pi$ and B^*K final states. On the other hand, if there is little mixing between $2^3S_1 - 1^3D_1$, the $B_J(5840)$ and $B_{sJ}(6114)$ resonances may be candidates for the $B(2^3S_1)$ and $B_s(1^3D_1)$ states, respectively.

The $B_J(5970)$ resonance may be assigned as the 1^3D_3 state in the B meson family, although it as a pure 2^3S_1 state cannot be excluded according to present experimental information. To clarify the nature of $B_J(5970)$, further observations of the $B\pi$ and $B^*\pi$ channels and a measurement of their partial width ratio are necessary. In the B_s family, the predicted mass $M \simeq 6067$ MeV and width $\Gamma \simeq 13$ MeV for the $B_s(1^3D_3)$ are consistent with the $B_{sJ}(6064)$ structure observed in the B^+K^- mass spectrum. However, the $B_s(1^3D_3)$ may not be the main contributor to the $B_{sJ}(6064)$ structure. If $B_{sJ}(6064)$ corresponds to $B_s(1^3D_3)$, another narrow structure around 6019 MeV coming from the $B^{*+}K^-$ decay should be observed in the B^+K^- mass spectrum, however, it was not seen at LHCb.

The narrow $B_{sJ}(6064)$ structure observed in the B^+K^- mass spectrum may mainly come from the resonance $B_{sJ}(6109)$ decaying into $B^{*+}K^-$. The $B_{sJ}(6109)$ resonance favors the assignment of the high mass $1D$-wave mixed state $B_s(1D_2')$ with $J^P = 2^-$. This state dominantly decays into B^*K channel with branching fraction about 95%, and the BK decay is forbidden. The other missing mixed state $B_s(1D_2)$ has a mass of $M \simeq 5973$ MeV and a width of $\Gamma \simeq 90$ MeV. It is most likely to be established in the B^+K^- mass spectrum through the $B^{*+}K^-$ decay with a missing photon from $B^{*+} \to B^+\gamma$. In the B-meson sector, two relatively broad mixed states, $B(1D_2)$ with $M \simeq 5973$ MeV and $B(1D_2')$ with $M \simeq 6067$ MeV, may be observed their main decay channel $B^*\pi$ with a larger data sample at LHCb.

Finally, it should be mentioned that the $B_J(5840)$ resonance may be a candidate of the $2S$-wave state $B(2^1S_0)$ as well. In this case, the $B\pi$ mode of $B_J(5840)$ is forbidden, which should be further confirmed in future experiments. In the B_s meson sector, our predicted mass and width for the $B_s(2^1S_0)$ state are $M = 5944$ MeV and $\Gamma \simeq 55$ MeV, respectively. The B^*K channel is the only OZI-allowed two body strong decay mode. The $B_s(2^1S_0)$ state should have large potentials to be seen in the $B^{*+}K^-$ channel since it has a fairly narrow width.

ACKNOWLEDGMENTS

Helpful discussions with Qi-Fang Lü and Ming-Sheng Liu are greatly appreciated. This work is supported by the National Natural Science Foundation of China (Grants No. U1832173, No. 11775078).

[1] P. A. Zyla *et al.* (Particle Data Group), Review of particle physics, Prog. Theor. Exp. Phys. **2020**, 083C01 (2020).
[2] V. M. Abazov *et al.* (D0 Collaboration), Observation and Properties of $L = 1B_1$ and B_2^* Mesons, Phys. Rev. Lett. **99**, 172001 (2007).
[3] T. Aaltonen *et al.* (CDF Collaboration), Measurement of Resonance Parameters of Orbitally Excited Narrow B^0 Mesons, Phys. Rev. Lett. **102**, 102003 (2009).
[4] T. Aaltonen *et al.* (CDF Collaboration), Observation of Orbitally Excited B_s Mesons, Phys. Rev. Lett. **100**, 082001 (2008).
[5] R. Aaij *et al.* (LHCb Collaboration), First Observation of the Decay $B_{s2}^*(5840)^0 \to B^{*+}K^-$ and Studies of Excited B_s^0 Mesons, Phys. Rev. Lett. **110**, 151803 (2013).
[6] V. M. Abazov *et al.* (D0 Collaboration), Observation and Properties of the Orbitally Excited B_{s2}^* Meson, Phys. Rev. Lett. **100**, 082002 (2008).
[7] T. A. Aaltonen *et al.* (CDF Collaboration), Study of orbitally excited B mesons and evidence for a new $B\pi$ resonance, Phys. Rev. D **90**, 012013 (2014).
[8] R. Aaij *et al.* (LHCb Collaboration), Precise measurements of the properties of the $B_1(5721)^{0,+}$ and $B_2^*(5747)^{0,+}$ states and observation of $B^{+,0}\pi^{-,+}$ mass structures, J. High Energy Phys. 04 (2015) 024.
[9] R. Aaij *et al.* (LHCb Collaboration), Observation of new excited B_s^0 states, arXiv:2010.15931.
[10] I. Belyaev, G. Carboni, N. Harnew, and C. M. F. Teubert, The history of LHCb, Eur. Phys. J. H **46**, 3 (2021).
[11] S. Godfrey and N. Isgur, Mesons in a relativized quark model with chromodynamics, Phys. Rev. D **32**, 189 (1985).
[12] J. Zeng, J. W. Van Orden, and W. Roberts, Heavy mesons in a relativistic model, Phys. Rev. D **52**, 5229 (1995).
[13] V. Kher, N. Devlani, and A. K. Rai, Spectroscopy, Decay properties and Regge trajectories of the B and B_s mesons, Chin. Phys. C **41**, 093101 (2017).
[14] D. Ebert, R. N. Faustov, and V. O. Galkin, Heavy-light meson spectroscopy and Regge trajectories in the relativistic quark model, Eur. Phys. J. C **66**, 197 (2010).
[15] J. B. Liu and C. D. Lü, Spectra of heavy-light mesons in a relativistic model, Eur. Phys. J. C **77**, 312 (2017).
[16] C. B. Lang, D. Mohler, S. Prelovsek, and R. M. Woloshyn, Predicting positive parity B_s mesons from lattice QCD, Phys. Lett. B **750**, 17 (2015).
[17] E. B. Gregory *et al.*, Precise B, B_s and B_c meson spectroscopy from full lattice QCD, Phys. Rev. D **83**, 014506 (2011).

[18] D. Jia and W. C. Dong, Regge-like spectra of excited singly heavy mesons, Eur. Phys. J. Plus **134**, 123 (2019).

[19] H. Y. Cheng and F. S. Yu, Masses of scalar and axial-vector B mesons revisited, Eur. Phys. J. C **77**, 668 (2017).

[20] M. H. Alhakami, Predictions for the beauty meson spectrum, Phys. Rev. D **103**, 034009 (2021).

[21] Y. Lu, M. N. Anwar, and B. S. Zou, How large is the contribution of excited mesons in coupled-channel effects?, Phys. Rev. D **95**, 034018 (2017).

[22] B. H. Yazarloo and H. Mehraban, Study of B and B_s mesons with a Coulomb plus exponential type potential, Europhys. Lett. **116**, 31004 (2016).

[23] M. Shah, B. Patel, and P. C. Vinodkumar, Spectroscopy and flavor changing decays of B, B_s mesons in a Dirac formalism, Phys. Rev. D **93**, 094028 (2016).

[24] M. Di Pierro and E. Eichten, Excited heavy-light systems and hadronic transitions, Phys. Rev. D **64**, 114004 (2001).

[25] Y. Sun, Q. T. Song, D. Y. Chen, X. Liu, and S. L. Zhu, Higher bottom and bottom-strange mesons, Phys. Rev. D **89**, 054026 (2014).

[26] S. Godfrey, K. Moats, and E. S. Swanson, B and B_s meson spectroscopy, Phys. Rev. D **94**, 054025 (2016).

[27] Q. F. Lü, T. T. Pan, Y. Y. Wang, E. Wang, and D. M. Li, Excited bottom and bottom-strange mesons in the quark model, Phys. Rev. D **94**, 074012 (2016).

[28] I. Asghar, B. Masud, E. S. Swanson, F. Akram, and M. A. Sultan, Decays and spectrum of bottom and bottom strange mesons, Eur. Phys. J. A **54**, 127 (2018).

[29] S. Godfrey and K. Moats, Spectroscopic assignments of the excited B-mesons, Eur. Phys. J. A **55**, 84 (2019).

[30] Z. H. Wang, Y. Zhang, T. H. Wang, Y. Jiang, Q. Li, and G. L. Wang, Strong decays of P-wave mixing heavy-light 1^+ states, Chin. Phys. C **42**, 123101 (2018).

[31] G. L. Yu and Z. G. Wang, Analysis of the excited bottom and bottom-strange states $B_1(5721)$, $B_2^*(5747)$, $B_{s1}(5830)$, $B_{s2}^*(5840)$, $B_J(5840)$ and $B_J(5970)$ in B meson family, Chin. Phys. C **44**, 033103 (2020).

[32] H. A. Alhendi, T. M. Aliev, and M. Savcı, Strong decay constants of heavy tensor mesons in light cone QCD sum rules, J. High Energy Phys. 04 (2016) 050.

[33] J. Ferretti and E. Santopinto, Open-flavor strong decays of open-charm and open-bottom mesons in the $^3P_0$ model, Phys. Rev. D **97**, 114020 (2018).

[34] Z. G. Wang, Strong decay of the heavy tensor mesons with QCD sum rules, Eur. Phys. J. C **74**, 3123 (2014).

[35] H. Xu, X. Liu, and T. Matsuki, Newly observed $B(5970)$ and the predictions of its spin and strange partners, Phys. Rev. D **89**, 097502 (2014).

[36] Z. G. Wang, Strong decays of the bottom mesons $B_1(5721)$, $B_2(5747)$, $B_{s1}(5830)$, $B_{s2}(5840)$ and $B(5970)$, Eur. Phys. J. Plus **129**, 186 (2014).

[37] J. M. Zhang and G. L. Wang, Strong decays of the radial excited states $B(2S)$ and $D(2S)$, Phys. Lett. B **684**, 221 (2010).

[38] Z. G. Luo, X. L. Chen, and X. Liu, $B_{s1}(5830)$ and $B_{s2}^*(5840)$, Phys. Rev. D **79**, 074020 (2009).

[39] P. Gupta and A. Upadhyay, Decay width and coupling constants of charm and bottom mesons, *Proc. Sci.*, Hadron2017 (2018) 025.

[40] P. Gupta and A. Upadhyay, Placing the newly observed state $B_J(5840)$ in bottom spectra along with states $B_1(5721)$, $B_2^*(5747)$, $B_{s1}(5830)$, $B_{2s}^*(5840)$ and $B_J(5970)$, Phys. Rev. D **99**, 094043 (2019).

[41] S. L. Zhu and Y. B. Dai, The Effect of B pi continuum in the QCD sum rules for the $(0^+, 1^+)$ heavy meson doublet in HQET, Mod. Phys. Lett. A **14**, 2367 (1999).

[42] A. H. Orsland and H. Hogaasen, Strong and electromagnetic decays for excited heavy mesons, Eur. Phys. J. C **9**, 503 (1999).

[43] G. L. Yu, Z. G. Wang, and Z. Y. Li, Strong coupling constants and radiative decays of the heavy tensor mesons, Eur. Phys. J. C **79**, 798 (2019).

[44] T. M. Aliev and M. Savc, Radiative decays of the heavy tensor mesons in light cone QCD sum rules, Phys. Rev. D **99**, 015020 (2019).

[45] L. F. Gan and M. Q. Huang, QCD sum rule analysis of semileptonic B_{s1}, B_{s2}^*, B_{s0}^*, and B_{s1}' decays in HQET, Phys. Rev. D **82**, 054035 (2010).

[46] B. Grinstein and J. M. Camalich, Weak Decays of Excited B Mesons, Phys. Rev. Lett. **116**, 141801 (2016).

[47] L. Y. Xiao and X. H. Zhong, Strong decays of higher excited heavy-light mesons in a chiral quark model, Phys. Rev. D **90**, 074029 (2014).

[48] H. X. Chen, W. Chen, X. Liu, Y. R. Liu, and S. L. Zhu, A review of the open charm and open bottom systems, Rep. Prog. Phys. **80**, 076201 (2017).

[49] A. Manohar and H. Georgi, Chiral quarks and the nonrelativistic quark model, Nucl. Phys. **B234**, 189 (1984).

[50] Z. P. Li, The Threshold pion photoproduction of nucleons in the chiral quark model, Phys. Rev. D **50**, 5639 (1994).

[51] Z. P. Li, H. X. Ye, and M. H. Lu, An Unified approach to pseudoscalar meson photoproductions off nucleons in the quark model, Phys. Rev. C **56**, 1099 (1997).

[52] Q. Zhao, J. S. Al-Khalili, Z. P. Li, and R. L. Workman, Pion photoproduction on the nucleon in the quark model, Phys. Rev. C **65**, 065204 (2002).

[53] X. H. Zhong and Q. Zhao, Strong decays of newly observed D_{sJ} states in a constituent quark model with effective Lagrangians, Phys. Rev. D **81**, 014031 (2010).

[54] X. H. Zhong, Strong decays of the newly observed $D(2550)$, $D(2600)$, $D(2750)$, and $D(2760)$, Phys. Rev. D **82**, 114014 (2010).

[55] X. H. Zhong and Q. Zhao, Strong decays of heavy-light mesons in a chiral quark model, Phys. Rev. D **78**, 014029 (2008).

[56] X. H. Zhong and Q. Zhao, Charmed baryon strong decays in a chiral quark model, Phys. Rev. D **77**, 074008 (2008).

[57] L. Y. Xiao and X. H. Zhong, Ξ baryon strong decays in a chiral quark model, Phys. Rev. D **87**, 094002 (2013).

[58] L. H. Liu, L. Y. Xiao, and X. H. Zhong, Charm-strange baryon strong decays in a chiral quark model, Phys. Rev. D **86**, 034024 (2012).

[59] H. Nagahiro, S. Yasui, A. Hosaka, M. Oka, and H. Noumi, Structure of charmed baryons studied by pionic decays, Phys. Rev. D **95**, 014023 (2017).

[60] Y. X. Yao, K. L. Wang, and X. H. Zhong, Strong and radiative decays of the low-lying D-wave singly heavy baryons, Phys. Rev. D **98**, 076015 (2018).

[61] K. L. Wang, Y. X. Yao, X. H. Zhong, and Q. Zhao, Strong and radiative decays of the low-lying S- and P-wave singly heavy baryons, Phys. Rev. D **96**, 116016 (2017).

[62] L. Y. Xiao, K. L. Wang, Q. f. Lü, X. H. Zhong, and S. L. Zhu, Strong and radiative decays of the doubly charmed baryons, Phys. Rev. D **96**, 094005 (2017).

[63] K. L. Wang, L. Y. Xiao, X. H. Zhong, and Q. Zhao, Understanding the newly observed Ω_c states through their decays, Phys. Rev. D **95**, 116010 (2017).

[64] M. S. Liu, K. L. Wang, Q. F. Lü, and X. H. Zhong, Ω baryon spectrum and their decays in a constituent quark model, Phys. Rev. D **101**, 016002 (2020).

[65] S. J. Brodsky and J. R. Primack, The electromagnetic interactions of composite systems, Ann. Phys. (N.Y.) **52**, 315 (1969).

[66] F. E. Close and L. A. Copley, Electromagnetic interactions of weakly bound composite systems, Nucl. Phys. **B19**, 477 (1970).

[67] F. E. Close and Z. P. Li, Photoproduction and electroproduction of N^* in a quark model with QCD, Phys. Rev. D **42**, 2194 (1990).

[68] Z. Li, Compton scattering and polarizabilities of the nucleon in the quark model, Phys. Rev. D **48**, 3070 (1993).

[69] Q. Zhao, Z. P. Li, and C. Bennhold, Vector meson photoproduction with an effective Lagrangian in the quark model, Phys. Rev. C **58**, 2393 (1998).

[70] Q. Zhao, Nucleonic resonance excitations with linearly polarized photon in $\gamma p \to \omega p$, Phys. Rev. C **63**, 025203 (2001).

[71] Q. Zhao, J. S. Al-Khalili, and C. Bennhold, Quark model predictions for K^* photoproduction on the proton, Phys. Rev. C **64**, 052201 (2001).

[72] M. S. Liu, Q. F. Lü, and X. H. Zhong, Triply charmed and bottom baryons in a constituent quark model, Phys. Rev. D **101**, 074031 (2020).

[73] Q. F. Lü, K. L. Wang, L. Y. Xiao, and X. H. Zhong, Mass spectra and radiative transitions of doubly heavy baryons in a relativized quark model, Phys. Rev. D **96**, 114006 (2017).

[74] F. E. Close, A. Donnachie, and Y. S. Kalashnikova, Radiative decays of excited vector mesons, Phys. Rev. D **65**, 092003 (2002).

[75] S. F. Chen, J. Liu, H. Q. Zhou, and D. Y. Chen, Electric transitions of the charmed-strange mesons in a relativistic quark model, Eur. Phys. J. C **80**, 290 (2020).

[76] W. J. Deng, H. Liu, L. C. Gui, and X. H. Zhong, Charmonium spectrum and their electromagnetic transitions with higher multipole contributions, Phys. Rev. D **95**, 034026 (2017).

[77] W. J. Deng, H. Liu, L. C. Gui, and X. H. Zhong, Spectrum and electromagnetic transitions of bottomonium, Phys. Rev. D **95**, 074002 (2017).

[78] Q. Li, M. S. Liu, L. S. Lu, Q. F. Lü, L. C. Gui, and X. H. Zhong, Excited bottom-charmed mesons in a nonrelativistic quark model, Phys. Rev. D **99**, 096020 (2019).

[79] T. Barnes, S. Godfrey, and E. S. Swanson, Higher charmonia, Phys. Rev. D **72**, 054026 (2005).

[80] E. Eichten, K. Gottfried, T. Kinoshita, K. D. Lane, and T. M. Yan, Charmonium: The model, Phys. Rev. D **17**, 3090 (1978); , Erratum, Phys. Rev. D **21**, 313 (1980).

[81] S. Godfrey and R. Kokoski, The properties of P wave mesons with one heavy quark, Phys. Rev. D **43**, 1679 (1991).

[82] S. Godfrey, Spectroscopy of B_c mesons in the relativized quark model, Phys. Rev. D **70**, 054017 (2004).

[83] E. Eichten and F. Feinberg, Spin dependent forces in QCD, Phys. Rev. D **23**, 2724 (1981).

[84] C.-H. Cai and L. Li, Radial equation of bound state and binding energies of Ξ^- hypernuclei, Chin. Phys. C **27**, 1005 (2003), http://cpc.ihep.ac.cn/article/id/e1b594c4-d44b-492f-adcf-7d53b4e5e56c.

[85] Q. Li, M. S. Liu, Q. F. Lü, L. C. Gui, and X. H. Zhong, Canonical interpretation of $Y(10750)$ and $\Upsilon(10860)$ in the Υ family, Eur. Phys. J. C **80**, 59 (2020).

[86] Q. Li, L. C. Gui, M. S. Liu, Q. F. Lü, and X. H. Zhong, Mass spectrum and strong decays of strangeonium in a constituent quark model, Chin. Phys. C **45**, 023116 (2021).

[87] R. Koniuk and N. Isgur, Baryon decays in a quark model with chromodynamics, Phys. Rev. D **21**, 1868 (1980); , Erratum, Phys. Rev. D **23**, 818 (1981).

[88] S. Capstick and W. Roberts, Quark models of baryon masses and decays, Prog. Part. Nucl. Phys. **45**, S241 (2000).

[89] L. A. Copley, G. Karl, and E. Obryk, Single pion photoproduction in the quark model, Nucl. Phys. **B13**, 303 (1969).

[90] R. Sartor and F. Stancu, Photodecay amplitudes in a flux-tube model for baryons, Phys. Rev. D **33**, 727 (1986).

[91] A. L. Licht and A. Pagnamenta, Wave functions and form-factors for relativistic composite particles. I, Phys. Rev. D **2**, 1150 (1970).

[92] G. Jaczko and L. Durand, Understanding the success of nonrelativistic potential models for relativistic quark-anti-quark bound states, Phys. Rev. D **58**, 114017 (1998).

[93] N. Isgur and M. B. Wise, Weak decays of heavy mesons in the static quark approximation, Phys. Lett. B **232**, 113 (1989).

[94] N. Isgur and M. B. Wise, Weak transition form-factors between heavy mesons, Phys. Lett. B **237**, 527 (1990).

[95] T. Matsuki, T. Morii, and K. Seo, Mixing angle between $^3P_1$ and $^1P_1$ in HQET, Prog. Theor. Phys. **124**, 285 (2010).

[96] F. E. Close and E. S. Swanson, Dynamics and decay of heavy-light hadrons, Phys. Rev. D **72**, 094004 (2005).

[97] T. Barnes, N. Black, and P. R. Page, Strong decays of strange quarkonia, Phys. Rev. D **68**, 054014 (2003).

[98] R. Akers *et al.* (OPAL Collaboration), Observations of $\pi - B$ charge-flavor correlations and resonant $B\pi$ and BK production, Z. Phys. C **66**, 19 (1995).

[99] S. Godfrey and K. Moats, Properties of excited charm and charm-strange mesons, Phys. Rev. D **93**, 034035 (2016).

[100] B. Chen, L. Yuan, and A. Zhang, Possible $2S$ and $1D$ charmed and charmed-strange mesons, Phys. Rev. D **83**, 114025 (2011).

[101] D.-M. Li and B. Ma, Implication of BABAR's new data on the $D_{s1}(2710)$ and $D_{sJ}(2860)$, Phys. Rev. D **81**, 014021 (2010).

[102] F. E. Close, C. E. Thomas, O. Lakhina, and E. S. Swanson, Canonical interpretation of the $D_{sJ}(2860)$ and $D_{sJ}(2690)$, Phys. Lett. B **647**, 159 (2007).

[103] H. Yu, Z. Zhao, and A. Zhang, Dynamical mixing between 2^3S_1 and 1^3D_1 charmed mesons, Phys. Rev. D **102**, 054013 (2020).

[104] B. Chen, X. Liu, and A. Zhang, Combined study of $2S$ and $1D$ open-charm mesons with natural spin-parity, Phys. Rev. D **92**, 034005 (2015).

[105] R. Aaij *et al.* (LHCb Collaboration), Observation of Overlapping Spin-1 and Spin-3 $\bar{D}^0K^-$ Resonances at Mass 2.86 GeV$/c^2$, Phys. Rev. Lett. **113**, 162001 (2014).

[106] R. Aaij *et al.* (LHCb Collaboration), Dalitz plot analysis of $B_s^0 \to \bar{D}^0K^-\pi^+$ decays, Phys. Rev. D **90**, 072003 (2014).